FACULTY OF SCIENCE
UNIVERSITY OF COPENHAGEN

,,,,

Master's thesis

Jonathan Winfield Rheinlænder

Interhemispheric climate variability in a pre-industrial control simulation of CCSM4

Department of Geophysics

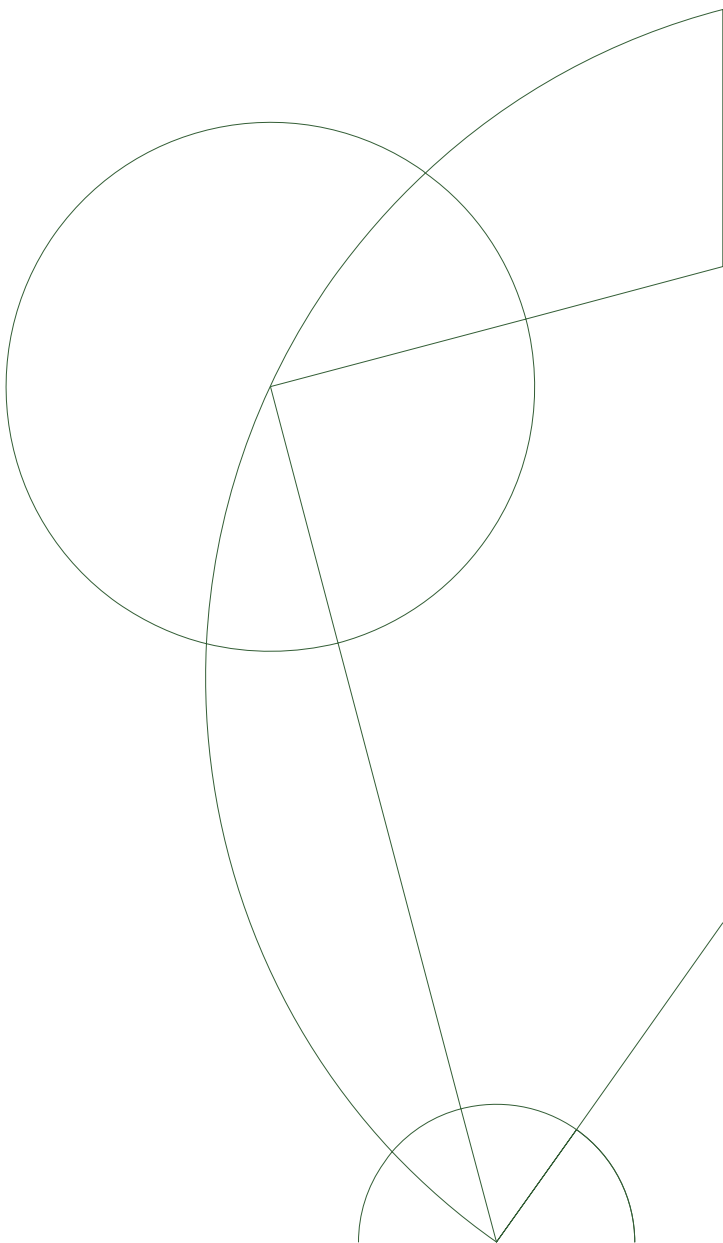

Prof. Markus Jochum

May 1st, 2015

Declaration of Authorship

Name of institute:
Niels Bohr Institute

Name of department:
Department of geophysics

Author:
Jonathan Winfield Rheinlænder

Titel:
Interhemisfærisk klima variabilitet i en koblet klimamodel

Title:
Interhemispheric climate variability in a pre-industrial control simulation of CCSM4

Subject description:
In a pre-industrial control simulation of CCSM4, a series of unforced and abrupt climate transitions in the North Atlantic is observed. The main goal of this thesis is to analyze and discuss the dynamics of the Southern Hemisphere response associated with these abrupt temperature changes in the Northern Hemisphere.

Academic supervisor:
Prof. Markus Jochum

Submitted: _____

Signed: _____

"The sea, once it casts its spell, holds one in its net of wonder forever."

Jacques Yves Cousteau

Resumé

Iskerner fra Grønland har afsløret en række bratte klimaforandringer, som fandt sted med jævne mellemrum gennem den sidste istid. De bratte temperaturskift under istiden kaldes ofte Dansgaard-Oeschger-begivenheder og har senere vist sig også at finde sted i Antarktis. Når man sammenligner iskernerne fra Grønland og Antarktis tegner der sig et mærkværdigt mønster, som viser at mens Grønland er varm så er Antarktis kold og omvendt. Dette unikke resultat viser et asymmetrisk forhold mellem Grønland og Antarktis, hvilket udgør et af de største mysterier inden for klimaforskningen. Nye observationer fra vest Antarktis, som netop er blevet afsløret, tyder kraftigt på at klimaændringerne på Grønland kommer forud for ændringerne på Antarktis, hvilket giver ny indsigt i de bagvedliggende mekanismer for koblingen mellem den nordlige og sydlige halvkugle under den sidste istid. En lang række studier har forslået at Dansgaard-Oeschger-begivenhederne må være udløst af en voldsom ændring af atmosfære- og havcirkulationen under istiden. I denne opgave præsenteres resultaterne fra en klima-model simulering der viser en række bratte klimaændringer i Nordatlanten, som følge af stokastiske processer i klimasystemet og som i høj grad minder om de temperaturændringer forbundet med Dansgaard-Oeschger-begivenhederne. Ud fra dette diskuterer vi, hvordan intern klimavaribilitet kan forklare det asymmetriske forhold mellem Grønland og Antarktis. Her finder vi, at disse skift er forårsaget af ændringer i det tropiske nedbørsmønster forbundet med El Nino/La Nina variabilitet. Disse ændringer er kommunikeret direkte til høje breddegrader i både den nordlige og sydlige halvkugle gennem atmosfæren og påvirker dermed den lokale cirkulation i de polare egne. I den sydlige halvkugle kommer dette blandt andet til udtryk gennem ændringer i dybvandsdannelsen omkring Antarktis. Dette viser sig at være en vigtig brik i det globale klimasystem, og kunne potentielt være en forklaring på det asymmetriske forhold mellem nordlige og sydlige høje breddegrader. Vores resultater tyder dog ikke på at temperaturen ændrer sig voldsomt på Antarktis, hvilket formentlig er på grund af den relativt lille ændring i den nordatlantiske varmetransport gennem havet. Ændringerne i havcirkulationen viser en svag opvarmning i ca. 1,000 meters dybde det nordlige Atlanterhav, som skyldes en svækkelse af den vind-drevne havcirkulation i Labradorhavet. Denne temperatur-anomali spredes gennem Atlanterhavet langs den vestlige randstrøm, men er drastisk svækket idet signalet når frem til det det sydlige Atlanterhav. Dette antyder at ændringerne i havcirkulationen, observeret i denne klimamodel, ligeledes er for svage til at påvirke temperaturerne på Antarktis.

...

Abstract

Climate reconstructions from ice core records in Greenland and Antarctica have revealed a series of abrupt climate transitions, showing a distinct relationship between northern and southern hemisphere climate during the last glacial period. It is generally believed that changes in the AMOC are responsible for this interhemispheric connection. This so-called *bipolar seesaw* mechanism, links the two hemispheres on centennial timescales and provides a framework for understanding the timing of the abrupt climate transitions during glacial times. The recent ice core records from West Antarctica (WAIS) points towards an atmospheric teleconnection as a possible trigger for the interhemispheric climate variability. This recent progress in paleoclimate observations, together with recent modelling efforts, calls for the classic bipolar seesaw theory to be revised.

In this modelling study, dynamics of abrupt climate transitions in an unforced control simulation of CCSM4 are explored. The model exhibits a series of abrupt changes in Greenland surface temperature triggered by internal climate variability, which closely resemble a Dansgaard-Oeschger event. Similar, but weaker changes are observed in the Southern Hemisphere synchronous with the abrupt changes in the Northern Hemisphere. We argue that both north and south high latitude climate variability is triggered by stochastic precipitation anomalies in the western tropical Pacific. The atmospheric wave guide then provides a fast communication pathway connecting the deep tropics and the polar regions. In the Southern Hemisphere this is manifested as a distinct pressure pattern over West Antarctica that strongly influences deep ocean convection in the Weddell Sea.

The ocean circulation response to the abrupt climate transitions show a characteristic asymmetric pattern in the subsurface temperature of the Atlantic, resembling a bipolar see-saw response. After an initial surface cooling in the subpolar gyre, the subsequent ocean adjustment is dominated by heat convergence at the subpolar-subtropical gyre boundary. This warming anomaly, located at mid-depth, spreads into the South Atlantic along the deep western boundary current, on time scales associated with slow advective processes. The anomaly is significantly reduced, as the signal reaches the South Atlantic midlatitudes, where further southward propagation is inhibited by the presence of the Antarctic Circumpolar Current (ACC). This suggest an essential role of the ACC in the setting the magnitude and time scale of the hemispheric response.

In line with a number of recent studies, the modelling evidence presented here shows that internal climate variability is a potential trigger for the abrupt climate transitions observed during the last glacial through the existence of a fast atmospheric teleconnection mechanism. Furthermore, our results show that propagation of an ocean temperature signal from the North Atlantic to Antarctica is hindered by the ACC, which presents an essential issue in the traditional *bipolar see-saw* mechanism.

Acknowledgements

I would like to acknowledge prof. Markus Jochum for supervising this thesis and including me in Team Ocean. This has truly been a great learning experience. My sincere appreciation goes to the Centre for Ice and Climate for providing such a friendly and dynamic environment. Here, a special thanks must go to Joel Pedro, Laura Herraiz, Hannah Kleppin and Helen Pillar for the enlightening discussions and great company. Your help and support is highly appreciated. Thanks to all the participants of the Southern Ocean workshop in Bergen (2-3 February, 2015) who have inspired many of the discussions herein. In particular, I'm deeply thankful for the work and support provided by Eric Steig (*University of Washington*) and Torge Martin (*Kiel University, Kiel, Germany*).

Finally, the author wish to acknowledge use of the Ferret program for analysis and graphics in this paper. Ferret is a product of NOAA's Pacific Marine Environmental Laboratory. (Information is available at http://ferret.pmel.noaa.gov/Ferret/)

...

Contents

List of Figures

Abbreviations

AABW	**A**nt**A**rctic **B**ottom **W**ater
ACC	**A**ntarctic **C**ircumpolar **C**urrent
AMOC	**A**tlantic **M**eridional **O**verturning **C**irculation
BLD	**B**oundary **L**ayer **D**epth
CAM	**C**ommunity **A**tmosphere **M**odel
CCSM4	**C**ommunity **C**limate **S**ystem **M**odel version 4
CLM	**C**ommunity **L**and **M**odel
CMIP	**C**oupled **M**odel **I**ntercomparison **P**roject
D-O events	**D**ansgaard-**O**eschger events
EDML	**E**PICA **D**ronning **M**aud **L**and
ENSO	**E**l **N**ino **S**outhern **O**scillation
EPICA	**E**uropean **P**roject for **I**ce **C**oring in **A**ntarctica
GISP-2	**Gr**eenland **I**ce **S**heet **P**roject 2
GRIP	**Gr**eenland **I**ce Core **P**roject
HE	**H**einrich **E**vents
IRD	**I**ce **R**afted **D**ebris
ITCZ	**I**nter-**T**ropical **C**onvergence **Z**one
LS	**L**abrador **S**ea
MIS3	**M**arine **I**sotope **S**tage 3
NA	**N**orth **A**tlantic
NADW	**N**orth **A**tlantic **D**eep **W**ater
NAO	**N**orth **A**tlantic **O**scillation
NGRIP	**N**orth **Gr**eenland **I**ce Core **P**roject
PNA	**P**acific-**N**orth **A**merican
POP	**P**arallel **O**cean **P**rogram

PSA	**P**acific-**S**outh **A**merican
SAG	**S**outh **A**tlantic **G**yre
SAM	**S**outhern **A**nnular **M**ode
SLP	**S**ea **L**evel **P**ressure
SPG	**S**ub-**P**olar **G**yre
SST	**S**ea **S**urface **T**emperature
WAIS	**W**est **A**ntarctic **I**ce **S**heet
WDW	**W**arm **D**eep **W**ater
WSBW	**W**eddell **S**ea **B**ottom **W**ater
WSCR	**W**eddell **S**ea **C**onvective **R**egion
WSDW	**W**eddell **S**ea **D**eep **W**ater
WTP	**W**estern **T**ropical **P**acific

Chapter 1

Introduction

One of the greatest mysteries throughout the history of our planet is the great ice ages, where our now so hospitable planet was transformed into a world of ice. Large ice sheets covered great parts of North America, Scandinavia and Greenland, resulting in dramatic drops in sea level which was about 120 m lower than today [Rahmstorf, 2007, Waelbroeck et al., 2002]. The great ice sheets that now cover Greenland and Antarctica holds information about the climate during the ice ages and it may prove as the key to understanding the future climate.

In the early 50's Danish geophysicist Willy Dansgaard discovered that the air bubbles trapped inside the ice offers a glimpse of the climate conditions in the past. He found that the isotopic composition of snow accumulated on the ice sheet could serve as a proxy for temperature at the time of deposition. Some 30 years later, this discovery lead to the first purely scientific ice core drilling project carried out in the southern part of Greenland and since then ice core research has been a fundamental pillar in modern paleoclimatology.

The ice core records from Greenland reveal remarkably detailed information about the climate conditions in the North Atlantic region during the last glacial period (60-27 ka). In this period the climate was much more variable compared with the warm and stable climate of the Holocene. The Greenland ice core records show evidence of rapid temperature fluctuations of $8 - 16°C$ in a matter of decades and resulted in climatic changes throughout most of the North Atlantic [Lang et al., 1999]. However, other paleoclimate records suggest that the dramatic changes observed in Greenland was not only confined to the North Atlantic, but had a global footprint. Oxygen isotope records of stalagmites

from Hulu Cave in China are remarkably similar to the Greenland ice core record [Wang et al., 2001]. The variations in $\delta^{18}O$ from the stalagmite records reflect a change in the East Asian Monsoon and propose a link between North Atlantic climate variability and meridional heat transport. Further evidence of teleconnections with North Atlantic climate during the last glacial period comes from marine records. Deplazes et al. [2013] analysed sediments from the Cariaco Basin and the northeastern Arabian Sea and found a close link between tropical and Greenland paleoclimate variability. This is supported by various studies of marine records (see Peterson et al. [2000] and Schulz et al. [1998]). There is, however, a slight bias in the spatial distribution of marine records towards the North Atlantic region.

The paleoclimate record show that there is global evidence of millennial-scale climate variability during the last glacial cycle, but the question remains if it is the same events we observe everywhere or are there regional differences? [Voelker, 2002] To answer this question, we must turn to climate models to explore the underlying mechanisms behind the hemispheric climate variability.

1.1 Advancements in paleoclimatology

During the glacial periods large temperature fluctuations was observed in the Northern hemisphere. The $\delta^{18}O$ record from Greenland ice cores reveals information about the multiple transitions from a glacial state to interstadial conditions. This was first discovered by the danish geophysicist Willy Dansgaard and his Swiss collegue Hans Oeschger from the University of Bern. During the last glacial cycle (60-27 ka) they found several of these abrupt climatic events, which later would be known as Dansgaard-Oeschger (D-O) events. These transitions from the cold stadials to the warmer interstadials are characterized by a rapid warming followed by a slow gradual cooling on time scales of a few centuries.

Since the first deep ice cores was drilled in the early 80's a vast amount work has been dedicated to understand the dynamics and asymmetry of the D-O cycles. Since then, there has been numerous ice core drilling projects in both Greenland and Antarctica. The ice core records from Antarctica revealed a surprising coupling between D-O events in Greenland and warming events in Antarctica during the last glaciation. However, from these early ice core studies it is only the large D-O events that are evident in the

Antarctic temperature record. These major Antarctic warming events are denoted A1 and A2 corresponding to D-O event 8 and 12 respectively. Due to the low resolution of the Antarctic record it was not possible, at this time, to ascribe all the observed D-O events to a corresponding Antarctic warming event. The lower resolution is primarily due to the lower accumulation rates in Antarctica compared to Greenland, which hugely dominates the uncertainty in Δage, which is a limiting factor when comparing the inter-hemispheric coupling on a millennial time scale. However, in a study by Blunier [1998], the phasing between Greenland and Antarctic records are assessed using a combination of the detailed ^{10}Be record and methane for synchronization. The synchronization suggested an out-of-phase relationship between the northern and southern hemisphere, with Antarctic warming leading Greenland temperatures by 1-2.5 kyr on average. This was in disagreement with the prevalent hypothesis at that time, that events in the North Atlantic are preceding those observed in the southern hemisphere [Bender et al., 1994]. The considerably large time lag observed between the northern and southern hemisphere favors a connection via the ocean, but the mechanisms are not well known. A better understanding of the dynamics that govern the north-south teleconnection would require that the common time scale of paleoclimatic records be known with a resolution better than 500 years or less [Stocker and Thomas, 1998]. This has been one of the major focus of attention in climate research during the last few decades.

1.1.1 EPICA Community paper

In one of the more recent studies by the EPICA Community members, the interhemispheric coupling is studied through high resolution ice core records from Antarctica and Greenland. The main focus is the climate variability and fast transitions in the $\delta^{18}O$ record during the last glacial cycle also known as Marine Isotope Stage 3 (MIS3). The climate in the North Atlantic sector is represented by the NGRIP core and the Southern Hemisphere is represented by an ice core from Dronning Maud Land (EDML). Due to the generally colder and dryer conditions in Antarctica the snow accumulation rates are generally much lower compared to Greenland and this makes it difficult to assign each D-O event to a corresponding Antarctic warming event. However, due to the coastal climate of the EDML core, the resolution is comparable to that of NGRIP. The EDML core was synchronized using the global CH4-record from the NGRIP, GRIP and GISP-2

ice cores and given on the new common age scale GICC05. The synchronization uncertainty for the EDML record in MIS3 ranges from 400 to 800 yr for all events, which is two to three times better than for other Antarctic sites. This is important because the uncertainty is much smaller than the duration of each warming or cooling event, and thus presented new information about the coupling between D-O events and Antarctic warmings.

The most prominent feature of the high resolution EDML ice core record is the well resolved climatic variability throughout MIS3. This enables a one-to-one coupling of glacial climate variability between the Northern and Southern Hemisphere, suggesting that each warming event on the southern hemisphere could be related to a corresponding D-O event in Greenland. There has been a general disagreement about whether the Greenland D-O events are leading the Antarctic warming events or vice versa. There is, however, an agreement that we need higher resolution of the ice core records to better understand the north/south coupling in terms of leads and lags. The phase relationship does not qualitatively explain what actually triggers the switch from stadial to interstadial, but the discussion is still important since it addresses the question of what mechanisms that could be responsible for the abrupt climate shifts.

1.1.2 Asynchronous climate variability and Heinrich events

Throughout the last glacial several events of fresh water discharge into the North Atlantic has been observed in deep ocean sediment cores. Rock debris deposited onto the fine grained sediments of the ocean floor bear witness of large iceberg surges originating from North America and reaching far into the North Atlantic. Thus, the ice rafted debris (IRD) observed in ocean sediment cores correspond to massive ice rafting events commonly known as Heinrich events. However, while the evidence of the HE is clear, the causes of the sudden ice sheet collapse are not fully understood. Was it an abrupt climatic change that caused the ice sheet to collapse or internal dynamics resulting in surging of the ice sheet? It is not clear if the periodic surges are direct consequences of internal climate variability i.e. linked to interconnections between atmosphere, ocean and ice. This remains one of the great challenges in modern palaeoceanography and there is still an ongoing debate about the role of Heinrich events in North Atlantic climate variability during the last glacial stage.

For many years it has been suggested that the ice-rafting events and the associated freshwater discharge into the North Atlantic is the direct cause of the abrupt temperature changes in Greenland through changes in the Atlantic Meridional Overturning Circulation (AMOC). This view is supported by modeling studies [Chiang et al., 2008, Liu et al., 2009] which show that the AMOC is highly the sensitive to freshwater input. The melting reduces deep-water formation resulting in a weakening the overturning circulation, thus leading to reduced poleward heat transport and cooling in the North Atlantic region. In these modeling experiments fresh water is dumped into the North Atlantic leading to a reduced deep water production and thus a weaker overturning circulation. However, the source of these fresh water perturbations are not yet fully accounted for, and it points out that we should take caution in how the model experiments are designed. In addition to this, there appears to be a growing consonance among climate scientists, that the Heinrich events cannot be used as triggers for D-O events.

The high resolution EDML record, which shows a one-to-one coupling of antipodal climate variability in Greenland and Antarctica, adds new information about how Heinrich events are related to the bipolar see-saw. During MIS3 there is a linear relationship between the amplitude of Antarctic warmings and the duration of the stadial in Greenland. Hence, the Antarctic warming rate and the accompanying interhemispheric heat flux is similar for all D-O events, which implies that the overturning rate remained practically unchanged throughout MIS3 [Barbante et al., 2006]. This challenges the notion of different overturning rates during Heinrich events. The observations, however, do suggest that Heinrich events have some kind of dynamical impact on antipodal climate variability. The largest Antarctic warming events A1 and A2 respectively coincide with anomalously big Heinrich events (H4 and H5). It has been suggested that the large freshwater flux, during these big Heinrich events, causes the restoring to be slower and the stadial period is prolonged in Greenland. Although, a clear relationship has been hard to establish and there is no direct evidence that the freshwater discharges into the North Atlantic is systematically concurrent with the onset of the stadials. Hence, the question of what triggers the D-O events remains.

1.2 Recent advancements: WAIS ice core drilling project

The phase relationship between Greenland and Antarctica has been subject to vigorous debate within the paleoclimate community since the coupling was first realized over two decades ago. Though much work has gone into disentangle the processes responsible for the fast transitions from stadial to interstadial conditions the question about the phase relationship would remain unresolved.

Recent advancements in Antarctic ice core drilling may add some important and groundbreaking information about the heavily disputed phasing between the Northern and Southern Hemisphere. In early June, 2014 I had the pleasure of meeting Bradley Markle, who was visiting Center of Ice and Climate from University of Washington. Bradley is involved in the West Antarctic Ice Sheet drilling project (WAIS) and he presented some very interesting new ice core data, which could be a milestone in paleoclimate research and adds new information about the mechanisms responsible for the rapid climate fluctuations that occurred in both hemispheres throughout the last glacial.

The WAIS project present the most recent deep ice core record from West-Antarctica, and it characterized by an exceptionally high resolution comparable to that of NGRIP. The climate conditions in the western part of Antarctica is generally more humid due to the coastal climate than central parts of the Antarctic ice sheet thus accumulation rates are much higher. High resolution methane record from NGRIP is used for synchronization. The uncertainties of Δage was reduced due to thicker annual layers in the ice core and through optimization of the firn densification model.

The new data from the WAIS project provides a revision of the relative timing between temperatures between Greenland and Antarctica during MIS3. Due to the high resolution, and the low uncertainty in Δage it possible to pinpoint the exact time when the temperature increases and the timing between antipodal climate events. They find that warming events in Antarctica lag Greenland by approximately 170 yr. The $\delta^{18}O$ record from NGRIP shows a rapid increase closely followed by an increase in methane concentrations. Interestingly, the methane concentrations, inferred from the Antarctic record, appears to change simultaneously to the changes in the Northern Hemisphere. This can be interpreted as a global reorganization of the atmospheric circulation. However, in Antarctica the temperature ($\delta^{18}O$) record, does not change before about 170 yr later, suggesting a lag relatively to changes in Greenland which is significantly shorter than what has previously been suggested. The results is a rather robust indication

that Greenland has been leading Antarctica during the last glacial period and is further supported by a rapid increase in the deuterium excess. These changes occur simultaneously with the changes in methane concentrations, which also means the same time as the abrupt shift in Greenland temperature. The deuterium excess record is thus, believed to be a proxy for past changes in the atmospheric circulation and further suggest that atmospheric changes in Antarctica preceded the shift in temperature. The 200-year lag suggested by these recent results favors a connection through the ocean, which operates on much longer timescales compared to the atmosphere. Hence, this indicates that changes in ocean circulation is an essential part of the mystery about the interhemispheric coupling.

1.3 Unraveling the mysteries of D-O events

The mechanisms responsible for the onset and termination of the D-O events and the coupling with Antarctic climate is one of the fundamental questions in paleoclimate research that still remains unanswered. Throughout the last couple of decades, evidence for D-O events has been growing, not only in the Northern Hemisphere, but observations suggest that the temperature fluctuations had a global impact. These widespread climatic events, that took place throughout the last glacial period, is now considered to be a well-known artifact of the climate system, although the driving mechanisms have yet to be studied in greater detail.

One of the greatest advancements in recent paleoclimatic research is the WAIS project and the results present a clear and robust indication that Greenland D-O events are leading Antarctic warming. The big question which still remains is how to get the signal from the Northern Hemisphere to the Southern Hemisphere. The leading hypothesis for the interhemispheric climate variability is connected to a slowdown of the deep water formation due to a freshwater discharge into the North Atlantic Ocean, affecting deep water formation. The source of this freshwater is still a controversial issue among climate scientists and especially the Heinrich events are heavily disputed. Nevertheless, it is generally accepted (Stocker and Thomas [1998], Blunier [1998], Margari et al. [2010] ect.) that the ocean must play a significant role in the onset of D-O events and in the connection between the climatic signals in the Southern and Northern Hemisphere. The general idea was proposed by Crowley [1992] and shows, that slowdown of the meridional

overturning circulation in the North Atlantic would lead to a reduced northward heat transport. Hence, the North Atlantic would tend to cool, while heat would accumulate in the South Atlantic. Here, the bipolar see-saw is manifested as an antiphase relationship between the north and the south, driven by changes in meridional heat transport. A similar hypothesis was proposed by [Broecker, 1998], relating the interhemispheric asymmetry to an alternation between enhanced deep-water formation in the North Atlantic and enhanced deep-water formation in the Southern Ocean (competition between AABW and NADW). According to this mechanism the seesaw pattern is driven by release of heat from the deep ocean to surface during deep-water formation. However, these ideas have since been met with skepticism e.g. [Wunsch, 2006] who question the notion that shifts in North Atlantic ocean circulation trigger D-O events in Greenland, given the weak contribution of the high latitude ocean to the meridional flux of heat. The fundamental point of the argument is that the atmosphere accounts for most of the total meridional heat transport in the ocean/atmosphere system. This is particularly evident in the high latitudes where the oceanic contribution is less than 25% of the atmospheric contribution [Wunsch, 2006]. Although heavily debated, the classic bipolar see-saw described in [Broecker, 1998, Crowley, 1992] seem to remain the widely-held view of abrupt climate change during the last glacial period

Stocker and Johnsen [2003] proposed an additional contribution to the classic bipolar see-saw theory where a heat reservoir is coupled to the original bipolar see-saw. In this *thermal bipolar see-saw*, the Southern Ocean acts as a heat reservoir, which allows for a significant improvement of the north-south correlation observed in the ice core records. Thus, the interhemispheric coupling occurs through a combination of the ocean and the atmosphere. Furthermore, it is suggested that coastal Kelvin and Rossby waves play a significant role in the adjustment processes and in the interhemispheric coupling. This view is supported by a later modeling study by [Chiang et al., 2008], which examines the response of North Atlantic climate following an abrupt freshwater discharge in a coupled model. They show that the initial adjustment is dominated by a fast atmosphere-surface ocean mechanism, resulting in a southward displacement of the tropical Atlantic ITCZ. More recently, this has been supported by a number of studies focused primarily on the atmospheric teleconnection in coupling North Atlantic and South Atlantic climate [Chiang et al., 2014, Lee et al., 2011]. Hence, surface ocean changes in the North Atlantic sector is shown to have a large impact on the global atmospheric circulation, which could explain the fast synchronous response in Greenland and Antarctica inferred from

the methane record from WAIS.

In recent years, there has been an increased focus on local climate variability as a trigger for the abrupt climate transitions in Greenland and Antarctica. Here, changes in sea ice is likely to play an important role as a strong feedback mechanism in high latitude climate. [Chiang and Bitz, 2005, Dokken et al., 2013] [Dokken et al., 2013] present in a recent study a novel mechanism for the abrupt D-O events caused by internal variability in the sea ice extent induced by subsurface warming in the Nordic Seas. This is supported by observational evidence from a new high-resolution deep ocean sediment core in the North Atlantic region. This theory is particularly attractive, since it does not depend on the relative timing of the Heinrich events, but is rather a consequence of internal ocean dynamics. Another illuminating example of how ocean-sea ice interactions can affect the climate on centennial scales is the fresh [Martin et al., 2015]. This is also among one of a number of studies following the recent trend focusing their attention on the Southern Ocean in driving modern and past climate variability. The study focus how internal variability of open ocean deep convection in the Weddell Sea impacts the strength of the Atlantic Meridional Overturning Circulation (AMOC), thus serving as a possible driver of the asynchronous relationship between the Northern and Southern Hemispheres. A key to understanding this mechanism is the interplay between the deep water formation around Antarctica and changes in the Southern Ocean sea ice cover via the so-called polynyas. A polynya is an area of open ocean enclosed within the perennial sea ice cover thus enabling a direct transfer of heat from the ocean to the atmosphere. Generally, deep water formation occurs at the continental shelf of Antarctica and is a major source of the world's bottom water. This convection is linked to the formation of cold, saline water in coastal polynyas around Antarctica. Coastal polynyas or latent heat polynyas are formed when katabatic winds from the ice sheet push newly formed sea ice away from the coast. The wind cools the surface layer of the ocean through the release of latent heat and evaporation which leads to enhanced sea ice formation and brine rejection. Through this densification process, the surface water will sink to the bottom following the continental slope and mix with the surrounding water to form Antarctic Bottom Water. However, polynyas can also form in mid-ocean regions and are commonly referred to as sensible heat polynyas. The Weddell Polynya [Gordon et al., 2007], which formed in the open ocean, is an example of a sensible heat polynya. Here, the polynya is formed when relatively warm water is injected into the surface layer causing the sea ice in the convective region to melt. The polynya is maintained by a continuous

supply of heat from below along with favorable atmospheric circulation inhibiting sea ice formation. When the heat reservoir is exhausted sea ice formation can resume and the polynya freezes over. Hence, the open ocean polynya is an effective way of ventilating the deep ocean and could potentially lead to changes in deep water formation. [Martin et al., 2015] shows the existence of a massive polynya in the Weddell Sea persisting on centennial timescales, which has a great impact on the formation of Antarctic Bottom Water (AABW) leading to enhanced AABW transport during the convective regime. This is balanced by a reduction in the southward transport of NADW. Hence, this relates back to the idea by [Broecker, 1998] where the bipolar see-saw is manifested as a competition between deep water formation in the North Atlantic and the Southern Ocean.

The general overview given above describes some of the different hypotheses that explain the asymmetric hemispheric coupling. We can summarize these mechanisms as follows:

- Changes in AMOC triggered by freshwater in the North Atlantic drives a see-saw response in the Southern Hemisphere. This is the original bipolar see-saw [Broecker, 1998, Crowley, 1992, Stocker and Johnsen, 2003]
- North Atlantic cooling/warming triggers an atmospheric teleconnection from high to low latitudes. The anomalous atmospheric circulation in the tropics trigger a response in the Southern Hemisphere. [Chiang et al., 2008, 2014, Chiang and Bitz, 2005, Lee et al., 2011]
- Trigger in the Southern Ocean due to internal climate variability. The signal is mediated through the ocean to the Northern Hemisphere by changes in the overturning circulation. [Martin et al., 2015]
- Perturbations in the tropical region lead to parallel changes in the Northern and Southern Hemispheres, through a fast tropical-polar teleconnection in the atmosphere. This readily explains the synchronous response in atmospheric circulation in Antarctica and Greenland, however the time-lag in Antarctic temperature must be explained by different processes.

In light of the recent observations from WAIS, it becomes clear that a revision of original bipolar see-saw theory is urgent. In this study we present a review of the prevailing hypotheses on the bipolar see-saw. We base our analysis on a pre-industrial climate

model simulation of the Community Climate System Model version 4 (CCSM4), which shows a series of abrupt climate transitions in the North Atlantic closely mimicking the transition from a cold stadial to a warm interstadial phase associated with D-O events. We split the following analysis into two main sections; Part I, where we focus on the atmospheric teleconnection through the tropics and part II where we focus on signal propagation in the Atlantic Ocean.

Part I represents a relatively unexplored part of the current paleoclimate modelling research on interhemispheric climate variability. Here, we are trying to answer the following question: *"Can stochastic climate variability, triggered in the tropical region, induce abrupt climate transitions in the Northern and Southern Hemisphere similar to the observed asynchronicity found in Greenland and Antarctic ice core records?"* Here, we focus on the atmospheric teleconnection from the tropics to high southern latitudes and explore how local changes in the atmospheric circulation can impact the open ocean deep convection in the Southern Ocean.

In the second part, we explore the adjustment of the Atlantic Ocean circulation and subsequent equatorwards progression of a temperature signal at mid-depth following an abrupt climate transition in the North Atlantic. Here, we are trying to understand how changes in the AMOC can influence Antarctic climate through the classic bipolar see-saw. This is going back to the original idea proposed by [Broecker, 1998, Crowley, 1992] about a "ocean bipolar see-saw" due to a reduction in the AMOC strength triggered by an abrupt changes in the North Atlantic.

Chapter 2

Model description and experimental design

2.1 Model description

The Community Climate System Model (CCSM4) is a state-of-the-art general circulation model with a fully coupled atmosphere, ocean, land and sea-ice system. The CCSM4 consist of four separate models each simulating the different components of the earth's climate system. These models represent the earth's atmosphere, ocean, land and sea-ice connected by a central coupler, which allows the different components to exchange heat, momentum and other physical properties. The atmosphere is simulated by the Community Atmosphere Model version 4 (CAM4) running with 2° horizontal resosultion and 26 vertical levels. The horizontal grid exists of 288×200 latitude/longitude equally spaced grid points, in both directions. Since the previous version (i.e. CAM3), significant changes have been made in the deep convection scheme of the atmospheric model. These changes have improved the distribution of tropical precipitation and with that a more realistic representation of El Niño-Southern Oscillation variability. The ocean component used in CCSM4 is the Parallel Ocean Program version 2 (POP2), with a 1° horizontal resolution and 60 unevenly spaced levels in the vertical. In the upper 200 m of the ocean, the thickness of the vertical layers is about 10 m and increases to 200-250 m for the deep layers. The higher vertical resolution in the upper layers is important to resolve the dynamics in the surface ocean which is an essential part of the

general ocean circulation. This includes, a better representation of vertical mixing and ocean dynamics associated with mechanical forcing (i.e. wind stress, tidal effects) at the surface. The Community Land Model version 4.0 (CLM4.0) is the land model used in CCSM4, representing the land surface processes including vegetation, land-use changes, river run-off, geochemical model ect. Finally, the sea-ice component in CCSM4 uses the Community Ice Code version 4, and uses the same horizonatal grid as the ocean component. One of the more notable improvements in the sea-ice component since CCSM3, is a better representation of sea ice concentration in the Arctic. The sea-ice component is of particularly interest to this study, since we are focusing on high latitude climate where sea-ice is an important feedback mechanism.

To summerize, the CCSM4 represents one of todays most advanced coupled climate models with a broad range of applications. The usage of the model has become widespread in the university community for climate research including studies of paleoclimate, present day climate and projections of future climate change. A full and comprehensive description of the different model components, notable improvements since the previous version and details on the preindustrial control run can be found in [Danabasoglu et al., 2011, Gent et al., 2011].

2.2 Experimental design

This study is motivated by a recent study by [Kleppin et al., 2015], who document a series of unforced climate transitions in the North Atlantic. These abrupt climate transitions occur in a pre-industrial control run of CCSM4, thus occuring with no external varying forcing, but rather triggered by stochastic climate variability inherent in the model. The results presented here proceed on the basis of the same 1,000-year CCSM4 integration analyzed in [Kleppin et al., 2015] featuring these abrupt changes in NA climate. The simulation used in this study is a pre-industrial control run with fixed forcing corresponding to pre-industrial conditions (i.e. year 1850). The model was initialized with fields from a previous coupled run and with incoming solar radiation set to 1360.9 W/m2 (at the TOA), and CO_2-levels set to 284.7 ppm. These forcings are kept constant during the whole integration. In the pre-industrial control run there is a small bias in the TOA mean heat balance, [Danabasoglu et al., 2011] with a small and fairly constant heat loss over the entire run, which primarily comes from the ocean component. This

means that there is a small drift in the ocean temperature in the control run [Gent et al., 2011]. Furthermore, since the model is initialized by observations there is a short spin-up period of a few hundred years in order for the system, including the upper ocean, to come into equilibrium. This is observed as an initial drift in the upper ocean of the South Atlantic, however this has no effect on the climate transitions in the NA. The objective of this study is to investigate the response of the coupled climate system in this pre-industrial control simulation of CCSM4. Here, we focus on how natural climate variability can trigger abrupt climate transitions in the Northern and Southern Hemisphere and we explore how changes in the general ocean circulation can affect Antarctic climate on a centennial time scale.

Chapter 3

Results

In this section we will present the results from the CCSM4 simulation. The first section will focus on some of the main characteristics of the simulation including the series of events leading to the abrupt climate transitions in the North Atlantic (NA). This analysis is motivated by the results presented in [Kleppin et al., 2015], who describes the processes of ocean-ice-atmosphere interactions responsible for the climate transitions. Hence, the main purpose of the first section is to illustrate potential triggers and feedback mechanisms involved in the rapid transitions in NA climate. The results from [Kleppin et al., 2015] leaves us with an obvious question. Is there a similar, but opposed response in Antarctica, yielding an evidence for a bipolar see-saw? And could this bipolar see-saw pattern be an inherent feature of our climate system triggered by stochastic climate variability? In the following sections we try to answer this question by exploring the Southern Hemisphere response and analyse the changes in global atmospheric circulation following an abrupt warming event in the NA.

3.1 Abrupt climate transitions in the North Atlantic

Here, we present a pre-industrial control simulation of CCSM4, where we find a series of spontaneous and unforced climate transitions in the North Atlantic. Throughout the 1000-year long integration we identify two different phases of NA climate mimicing the stadial-interstadial transitions during the last glacial. The cold phase is characterized by low temperatures over Greenland and pronounced advance of sea ice in the Labrador Sea and the warm phase is associated with low sea ice concentrations along with anomaously high temperatures over the NA. This is illustrated in figure 3.1 that shows the annual maximum sea ice concentration in the Labrador Sea and annual mean surface temperature averaged over Greenland. This reflects the different phases of NA climate, where low (high) concentrations of sea ice are associated with a warm (cold) NA phase respectively. Here, we observe two gradual transitions from a warm towards a cold NA state with an abrupt warming event separating the two cold phases. These transitions represents a strong feedback mechanism through ocean-ice-atmosphere interactions, which we will describe in the following.

During the first transition from a warm NA phase (years 50-250) to a cold phase (years 400-550) we observe a dramatic increase in sea ice cover in the Labrador Sea and a decrease in temperature over most of the NA and Greenland. Over the Labrador Sea temperaure decreases by up to $10°C$, but the response is weaker and more widespread in the rest of the North Atlantic region. To understand these changes in sea ice and Greenland temperature, we focus on the series of events leading up to the NA cold phase. During the initial part of the transition towards the cold phase (year 300-320), an anticyclonic sea level pressure anomaly evolves over Iceland, moving westward into the Labrador Sea. This resembles the charateristics of a negative phase of the North Atlantic Oscillation (NAO) and is also coherent with anomalous SST and convective precipitation in the tropical Pacific (i.e. ENSO-variability). The increased SLP over the SPG region, corresponding to a weakening of the cyclonic (anti-clockwise) circulation, results in a decrease in the wind stress curl by 10% relatively to the NA warm phase (year 50-250). This reduces the surface heat flux above the Labrador Sea thus establishing a cold core anomaly centered over the entire SPG. This allows sea ice cover to extend and helps to sustain the anomalous low SLP over the LS thus contributing to further weakening of the gyre circulation. The ocean circulation changes associated with the

reduced SPG circulation is a direct consequence of a slowdown of the Sverdrup transport due to the reduced wind stress curl and the changes in bouancy forcing. This contraction of the SPG reduces the advection of warm and high-salinity subtropical waters into the North Atlantic, and reduces the advection of salt into the Labrador Sea. This region is one of the primary sources of deep water formation, and is highly sensitive to changes in salinity. Here, we find that the reduction in salinity partly inibits deep convection in the LS, which tends to amplify the cooling around Greenland due to reduced heat transport by the AMOC that weakens by 3-4 Sv. The results from [Kleppin et al., 2015] show, that all atmospheric parameters are leading changes in the SPG circulation, suggesting that the weakening of the gyre circulation is driven by the anomalous atmospsheric conditions. The key results of this analysis show that the transition towards the cold NA phase is preceded by an abrupt decrease in precipitation over the western tropical Pacific, indicating a shift to predominantly El Niño type conditions. This suggest a dominant role for tropical climate variability in providing the initial trigger for the NA climate fluctuations. Hence, we can separate the series of events, associated with the

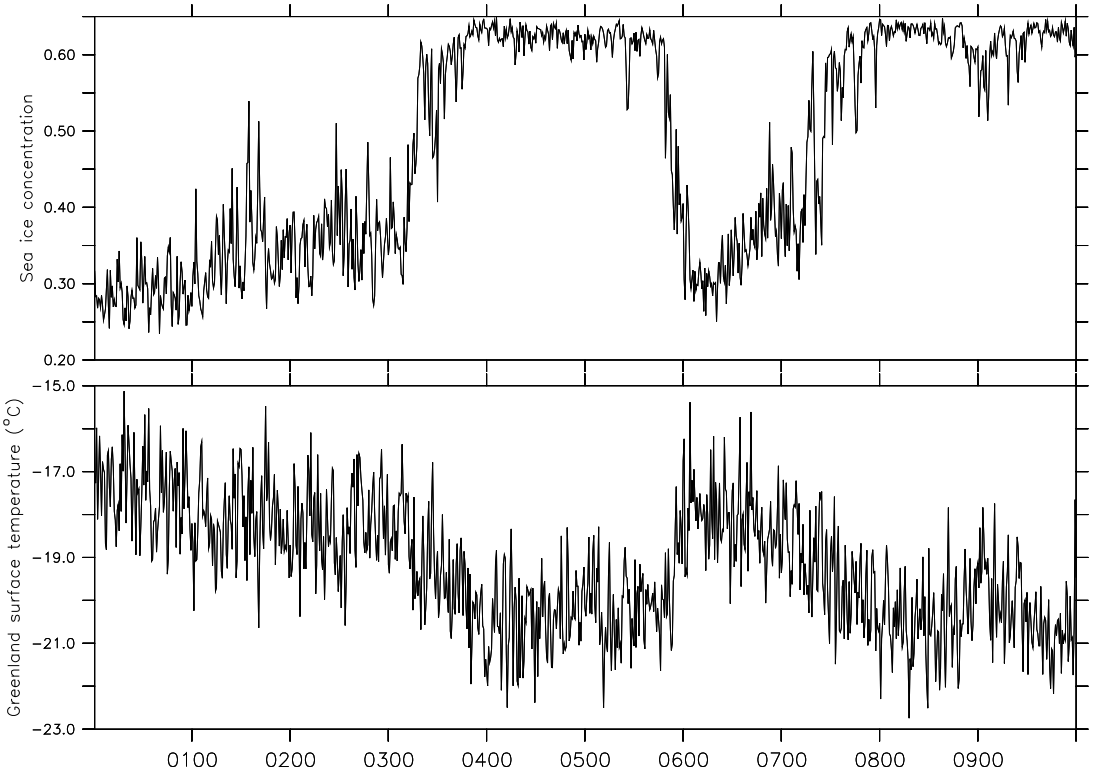

Figure 3.1: *Top:* Annual maximum of sea ice concentration in the Labrador Sea averaged from $65° - 45°W$ and $50° - 70°N$. *Bottom:* Greenland annual mean surface temperature [°C] averaged from $55° - 15°W$ and $65° - 80°N$

NA climate transition, into two parts. An initial trigger, in the form of a stochastic precipitation anomaly in the tropical Pacific, which induces a persistent SLP anomaly over the subpolar gyre. This then constitutes an atmospheric teleconnection between the tropics and northern high latitudes induced by ENSO variability and triggers a positive feedback loop, through weakening of the SPG circulation and subsequent increase in sea ice cover in the LS. Here, the positive feedback mechanism associated with the sea ice lead to an amplification of the temperature response over Greenland, and illustrate the significance of a positive feedback mechanism to amplify the initial response. These model results exhibit a striking similarity with the abrupt temperature variations during D-O events and present a basis for understanding the key dynamics causing the abrupt climate transitions related to D-O events. In this unforced model simulation these transitions arises due to stochastic climate variability in the tropics and is communicated to northern high latitudes through an atmospheric teleconnection. In the following sections we explore how the stochastic climate variability in the tropics might exhibit a similar teleconnection between the tropics and southern high latitudes and show how this could influence Antarctic climate.

3.2 The existence of a teleconnection between the tropics and southern high latitudes

In the remaining sections we primarily focus on the Southern Hemisphere response motivated by the abrupt changes observed in the North Atlantic. Here, we focus on the abrupt warming event in the North Atlantic, which occur at the terminus of the cold state and trigger the 2nd North Atlantic warm phase (see figure 3.1). The abrupt warming event, punctuating the cold phase, is particularly interesting because it mimics the transition into an interglacial state associated with a D-O event and represents a relatively unexplored part of the current modelling studies. Here, we analyze first the global changes in climate associated with the abrupt warming event, which provides a basis for understanding the atmospheric circulation changes in the Southern Hemisphere and the relationship with tropical climate variability, which we explore in detail later. Here, we focus primarily on changes in precipitation, sea level pressure and temperature where the main goal is to identify patterns of atmospheric changes in the Southern

Hemisphere that might be related to the anomalous precipitation in the western tropical Pacific.

3.2.1 Global changes in precipitation, sea level pressure and temperature

Figure 3.2a shows the difference in precipitation between the 2nd warm phase and the cold phase. All quantities have been deseasonalized with a 12-month running mean and the anomalies are calculated using the average of the first 50 years of the warm phase (years 600-650) with respect to the cold phase (years 400-550) preceding the abrupt warming. The anomalies thus illustrates the spatial extent of the immediate response from an abrupt warming in the North Atlantic. The abrupt warming event around year 600, is followed by relatively stable and warm conditions for about 5 decades. This is then followed by a decreasing trend in Greenland surface temperature leading to the transition into the 2nd cold phase around year 720, and accompanied by a rapid expansion of sea ice. Here, we are mainly interested in the effects on the atmospheric circulation associated with the abrupt warming event in the NA, which is why, we only consider the first 50 years of the warm phase.

The global precipitation changes are relatively small in magnitude $\leq$ 1mm/day, which is likely due to the stochastic nature of the model simulation, but are consistent with what we might expect from El Niño/La Niña variability [nas]. The precipitation pattern in the tropical Pacific resembles the signature of a negative ENSO-phase with positive precipitation anomalies centered over the western equatorial Pacific and negative precipitation anomalies over the central and eastern part of the tropical Pacific. This pattern is opposed to the precipitation pattern associated with the cooling event in the North Atlantic, which we discussed in section 3.1. Here, we argued that the cooling event is analogous to a shift towards El Niño conditions, with drying in the western Pacific and increased precipitation in the eastern Pacific. This suggests that the abrupt warming event in the NA is associated with La Niña conditions, thus supporting the idea that the climate transitions occurring in the NA are directly associated with precipitation changes in the equatorial Pacific (i.e. ENSO-variability). An important note here is that the amplitude and time scale of the precipitation anomalies are quite different from an ENSO-event. However, we simply note that the observed pattern closely resembles

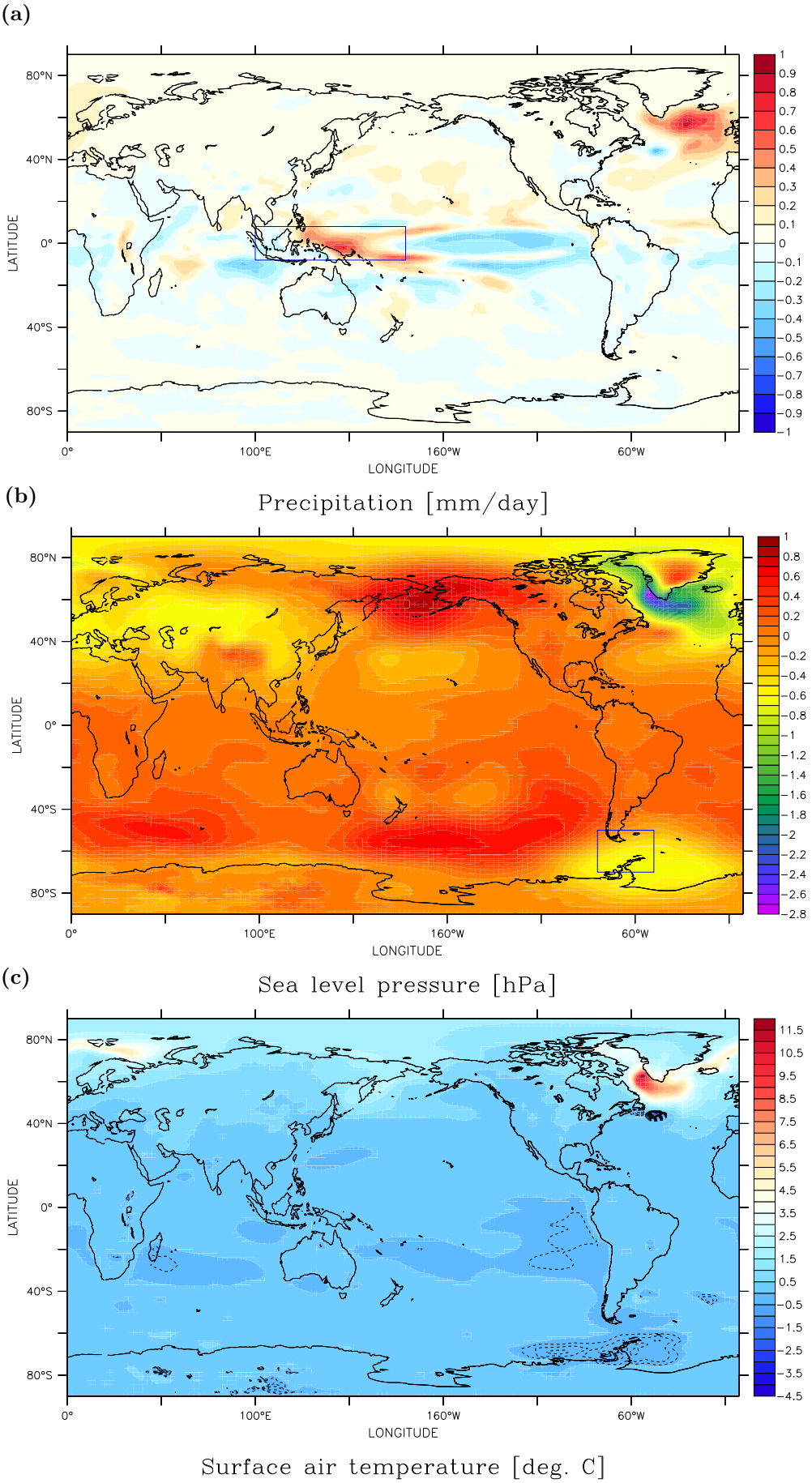

Figure 3.2: Global response in precipitation [mm/day] (a), sea level pressure [hPa] (b) and surface temperature [°C] (c) between years 400-550 (corresponding to NA cold state) and 600-650 (corresponding to the 2nd NA warm state). The area outlined by the blue box in the top and the middle panel represents the western tropical Pacific and the southern South America/Antarctic Peninsula respectively.

the cold and warm phases of ENSO, though the underlying dynamics might be slightly different. [Barsugli and Sardeshmukh, 2002] show that ENSO-events are closely linked to variations in tropical Pacific SST, reflecting an ocean-atmosphere interaction that drives a zonal shift in the precipitation patterns. Variability in tropical SST during cold and warm phases of ENSO, results in a shift in deep convection in the tropical Pacific with increased upper level divergence over the SST anomaly. This implies that relatively small changes in tropical SST can have a rather strong impact on precipitation causing a ripple effect throughout the mid- and high latitudes. Leading up to the abrupt warming event, there is a decreased variance in Niño 3.4 ($5°N - 5°S, 170° - 120°W$) SST variability from $\sigma^2 = 2.5$ in the cold phase to $\sigma^2 = 1.8$ in the warm phase [Kleppin et al., 2015]. This suggest a transition to predominantly La Niña conditions characterized by a sudden increase in precipitation over the western tropical Pacific region (outlined by the blue box in figure 3.2a).

Figure 3.2b shows the strong negative SLP anomaly centered over the southeastern tip of Greenland associated with the anomalous precipitation pattern in the tropical Pacific. In the Southern Hemisphere, the SLP anomalies are generally much smaller in amplitude. However, a relatively strong cyclonic pressure anomaly of 0.7hPa is centered over the Antarctic Peninsula and the western part of the Weddell Sea, between $50° - 60°W$ and $50° - 70°S$. The SLP anomaly has the same sign as the pressure pattern in the Northern Hemisphere, but the magnitude is significantly smaller. However, this matches with current observations, indicating that the northern high latitudes is generally more sensitive to tropical forcing during El Niño/La Niña events [Trenberth et al., 1998]. This interhemispheric asynchronicity is also evident in the surface temperature anomalies (figure 3.2c). In the NA, the greatest temperature increase is observed in the Labrador Sea with a warming of about 12°C, which can be attributed to the abrupt retreat of sea ice and increased ocean-atmosphere heat flux. Over Greenland, the temperature response is slightly weaker, where temperatures have increased locally by up to $4 - 5$°C relatively to the cold phase. In Antarctica however, the temperature variations are much weaker and more spatially variable compared to the changes in the North Atlantic. The strongest signal in the Southern Hemisphere temperature response is a weak cooling (about $0.3 - 1$°C) over the Antarctic Peninsula associated with the anomalous SLP pattern, while East Antarctica shows a general warming of less than 1°C, reflecting a predominantly in-phase relationship with Greenland temperature anomalies. The anomalous patterns of SLP and temperature which occur both around Greenland and

Antarctica suggest some kind of interhemispheric connection between the atmospheric circulation anomalies in the northern and southern high latitudes during the abrupt climate transitions. Here, the anomalous precipitation pattern in the equatorial Pacific associated with ENSO-variability, appears to be a precursor to the atmospheric circulation changes in both the Northern Hemisphere and the Southern Hemisphere. This is indicative of an atmospheric teleconnection through stochastic climate variability in the western tropical Pacific linking Greenland and Antarctic climate. The results presented here suggest that anomalous SST's and corresponding changes in the precipitation pattern in the tropical Pacific region, plays a key role in providing the triggering mechanism for the circulation anomalies in northern and southern high latitudes. In the following, we give a more detailed analysis of the Southern Hemisphere circulation response and the coupling with the tropical precipitation anomalies.

3.2.2 Tropical-high latitude teleconnection

The SLP anomalies throughout the Southern Hemisphere resembles the spatial extent associated with a Pacific-South American (PSA) pattern. This is one of the dominant modes of Southern Hemisphere climate variability and can arise naturally through atmospheric dynamics as well as in response to heating ipc. The Pacific-South American (PSA) pattern, which is analogous to the Pacific-North American (PNA) pattern in the northern hemisphere, is a great example of the existence of a meridional teleconnection acting through the large scale atmospheric wave guide. A large number of studies, have shown that this wave response can be triggered by tropical forcing and thus presents a very effective way of communicating tropical climate variability to middle and high latitudes. [Trenberth et al., 1998] show that the tropical heating, which could be associated with ENSO, and anomalous upper tropospheric divergence generates a Rossby wave response, with the wave energy propagating in a southeasterly direction throughout the troposphere from the source region in the tropical Pacific. In figure 3.2b, we identify this as a wave-like pattern of alternating high and low pressure anomalies, which appear to emanate from the subtropical western Pacific propagating towards West Antarctica. The southernmost cell of the wave train is an anomalous low centered over the Antarctic Peninsula and covering the entire Atlantic sector of the Southern Ocean (blue box in figure 3.2b). From West Antarctica the wave train extends into the South Pacific where a large positive SLP anomaly is present. The response is weaker as we move closer to the

center of action in the tropical Pacific. Hence, this resembles a classic stationary Rossby wave response to tropical SST forcing with a poleward intensification of the pressure anomalies. The Rossby wave response can be considered in terms of conservation of potential vorticity and results from displacement of isentropic surfaces (or: geopotential height surfaces, vorticity gradients) in the upper troposphere by strong vertical motion [Hoskins and Karoly, 1981]. This excites the barotropic wave mode and acts as a forcing on the barotropic vorticity equation, which responds by dispersion of Rossby waves into middle and high latitudes. Thus, the relatively fast propagation speed of the barotropic Rossby wave enables a fast communication between the tropical Pacific and southern high latitudes. Observational studies show that Southern Hemisphere response to tropical forcing are generally weaker and more variable compared to the counterpart in the Northern Hemisphere [Karoly, 1989, Vanloon and Shea, 1985]. This could explain the observed difference in magnitude we find between the Greenland and Antarctic climate response (see figure 3.2b). An important key to understanding this asynchronicity, is the inter-annual evolution of SST anomalies in the central tropical Pacific during an ENSO event described in [Karoly, 1989]. In the developing stage of an ENSO event, which typically occurs during SH winter (JJA), is characterized by weak and geographically variable SST anomalies in the central equatorial Pacific. As the ENSO event progresses the SST anomalies become more pronounced and during the mature stage of an ENSO event the region of maximum convective activity is shifted eastward into the central and eastern Pacific (El Niño) and towards the western Pacific and Indonesia during the negative phase of ENSO (La Niña). Throughout the midlatitudes, a wavetrain pattern extends from the central tropical Pacific across the North Pacific and North America. This northeastward arching wave signal is often referred to as the Pacific North-American pattern (PNA). Hence, during the early stage of an ENSO-event in the SH winter the circulation anomalies are weak, but exhibit a weak wavelike structure extending eastward and poleward. In the following northern hemisphere winter, in the mature stage of the ENSO-event, a strong wavetrain pattern extending across the North Pacific to North America exists. The associated circulation anomalies in the Northern Hemisphere high latitudes are stronger and more geographically constrained. In the Southern Hemisphere, the anomalies are also larger than the preceding winter. This furthermore demonstrates that the teleconnection pattern and the associated high latitude circulation anomalies are most pronounced in the winter hemisphere [Horel and Wallace, 1981]. This atmospheric teleconnection has been supported by extensive observational

and modeling studies, and is now widely accepted as one of the primary coupling mechanism between the tropics and high latitude and in driving large scale climate variability in the Northern and Southern Hemisphere.

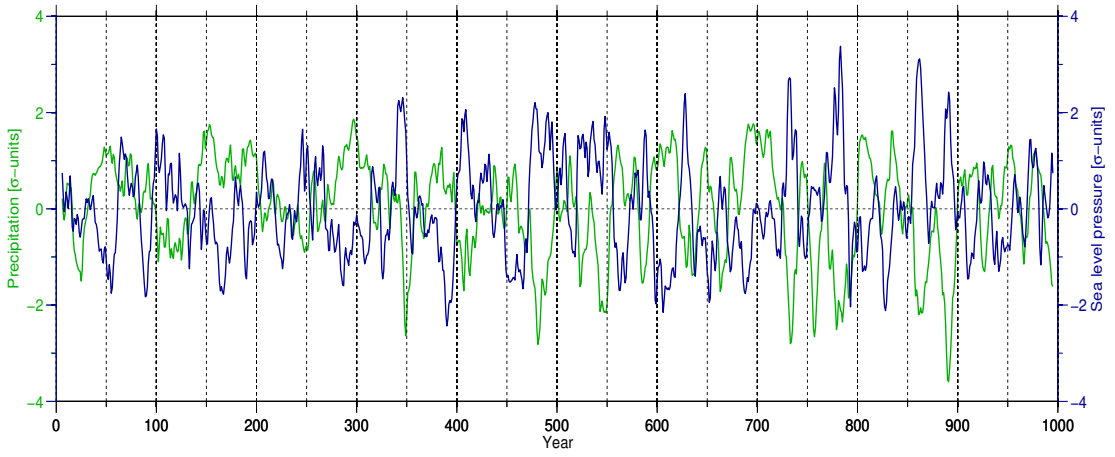

(a)

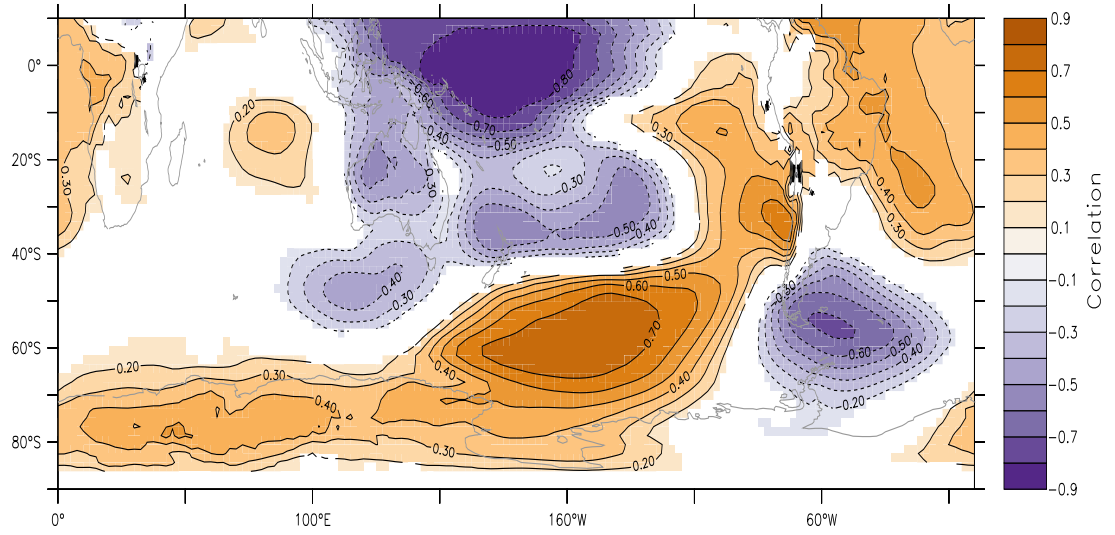

(b)

Figure 3.3: a Precipitation (green) and sea level pressure (blue) anomalies (unit variance) averaged over the western tropical Pacific ($100° - 180°E$ and $8°S - 8°N$) and from $50° - 60°W$ and $50° - 70°S$ respectively. A 10yr running mean is applied to filter out interannual variability. b Spatial correlation between precipitation anomalies averaged over the western tropical Pacific and Southern Hemisphere sea level pressure anomalies corresponding to the transition from the cold NA phase to the warm phase (i.e. year 400 to 650). Significant correlation is calculated using a 2-sided t-test and regions are only shaded if the correlation is significant on the 95% level.

The PSA pattern, describes an out-of-phase relationship between SLP anomalies in the South Atlantic sector and anomalous precipitation in the western tropical Pacific. This anti-phase relationship is illustrated in figure 3.3a, which shows the time series of the

relative changes in precipitation in the WTP and the associated SLP averaged over the South Atlantic sector (cf. blue box in figure 3.2b). We particularly note a relatively strong negative relationship ($\rho = -0.68$ with $p << 0.05$), suggesting a strong anti-correlation between SLP and tropical precipitation. The precipitation anomalies in the WTP occur simultaneous or previous to changes sea level pressure in the South Atlantic sector, which matches with the result from [Kleppin et al., 2015] and agrees well with the theoretical understanding of the Rossby wave response. The relationship shown in figure 3.3a demonstrates a tropical-extratropical teleconnection triggered by tropical SST forcing, which allows for a virtually instantaneous response to tropical forcing. The wave-like structure associated with the atmospheric teleconnection is illustrated in figure 3.3b, that shows the spatial correlation between precipitation anomalies in the western tropical Pacific and sea level pressure across the Southern Hemisphere over the period from year 400 to 650. Here, values are only shaded if the correlation with WTP precipitation is significant at the 95% level, based on a 2-sided Student's t-test. A pattern of high negative correlation is found centered over the southern tip of South America and agrees well with the anomalous SLP pattern observed in figure 3.2b. The correlation pattern of alternating anomalies linking the western Pacific to the South Atlantic sector is indicative of a stationary Rossby wave response discussed previously.

3.2.3 Impacts on Antarctic climate

The previously proposed teleconnection mechanism, predicts a significantly stronger response in the northern high latitudes which is consistent with the results showing that changes in the Southern Hemisphere are significantly smaller than those observed in the Northern Hemisphere. Here, we focus in detail on the atmospheric response in the southern high latitudes and explore how the tropical-polar teleconnection is manifested in Antarctica and the surrounding ocean. In figure 3.4a and 3.4b we show the changes in temperature, pressure and wind in the south polar region associated with the abrupt climate transition in the North Atlantic. Thus, the atmospheric circulation anomalies are similar to those shown in figure 3.2b, but shown explicitly for Antarctica for greater detail. Here, we only plot the anomalies if the difference is significant at the 95% confidence level. The significance test is based on a standard 2-sided t-test for comparing two samples corresponding to the warm phase (model year 600-650) and cold (model year 400-550). We apply a 10-year running mean to both samples and adjust the number

of degrees of freedom relatively to the running mean. We speculate, however, that we might be slightly overestimating the significance due to the smoothing. To test if the smoothing, induced by the running mean, could inflate the significance of the results, we tried a slightly different approach based on binning the data. Here, we bin the data into 10-year means and calculate the statistics based on the binned data and adjust the number of degrees of freedom to reflect the number of bins. The result (not shown) from this alternative method was generally consistent with the previous analysis (i.e. using the running mean), implying that the temperature anomalies shown in figure 3.4a and wind-stress changes in figure 3.4b are a relatively robust feature of the Southern Hemisphere climate response.

One of the prominent features of the PSA pattern in the Southern Hemisphere circulation is an out-of-phase relationship between the pressure and surface temperature anomalies between the Bellingshausen-Amundsen sector and the Weddell Sea (*i.e. Antarctic Dipole*). However, the SLP response in the southern high latitudes, illustrated by the overlaying contours in figure 3.4a, is dominated by an anomalous low covering the Pacific and Atlantic sector of the Southern Ocean including the peninsula and continental West Antarctica. Central and East Antarctica, however, shows a weak, but positive SLP anomaly indicating a "dipole" response between East and West Antarctica. However, we note that this is not a perfect PSA pattern, however the related changes in Antarctic temperature and wind-stress are similar to those associated with a PSA pattern. This apparently asynchronous response is also reflected in the surface temperatures, which shows cooling in West Antarctica while East Antarctica is warming. Warming is strongest (0.75°C) in East Antarctica and extends into the Southern Ocean. A relatively weak cold anomaly (< 1°C) is found in the Weddell Sea, Ross Sea and continental West Antarctica and is related to the cyclonic pressure anomaly centered over the peninsula. The wind-stress anomalies associated with the cyclonic SLP anomaly centered over the Antarctic Peninsula, show an anomalous cyclonic circulation, with offshore winds in the Bellingshausen Sea and onshore winds in the Weddell Sea. This could explain the observed negative temperature anomalies in this region due to advection of cold air from the Antarctic continent. The positive surface temperature anomalies in large parts of the Southern Ocean coincide with a strengthening of the circumpolar westerlies. An anomalous southward wind stress brings more warm air from the tropical Atlantic to higher southern latitudes and is then advected by the mean westward flow leading to

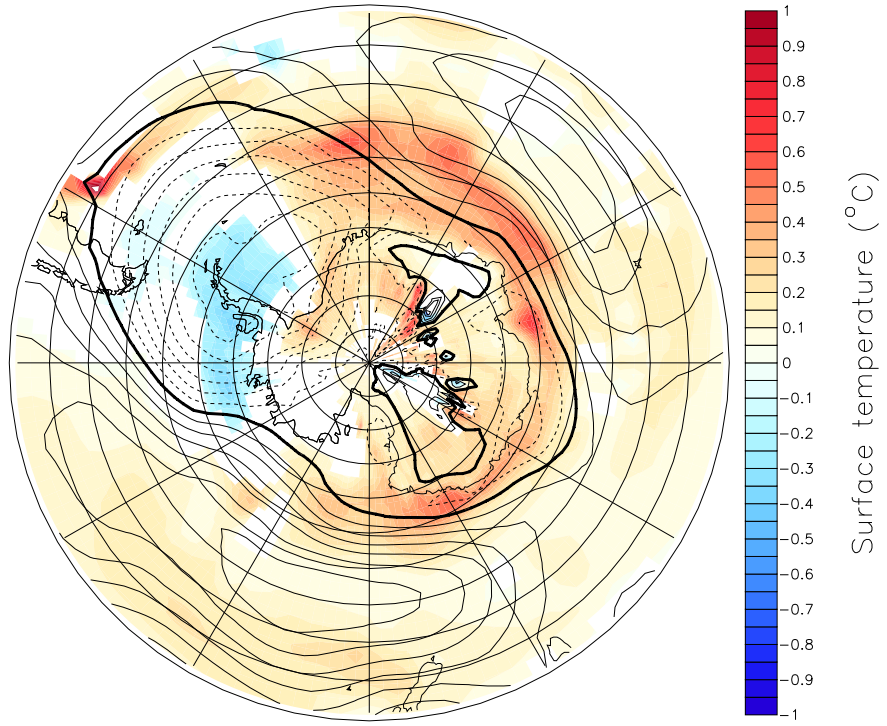

(a)

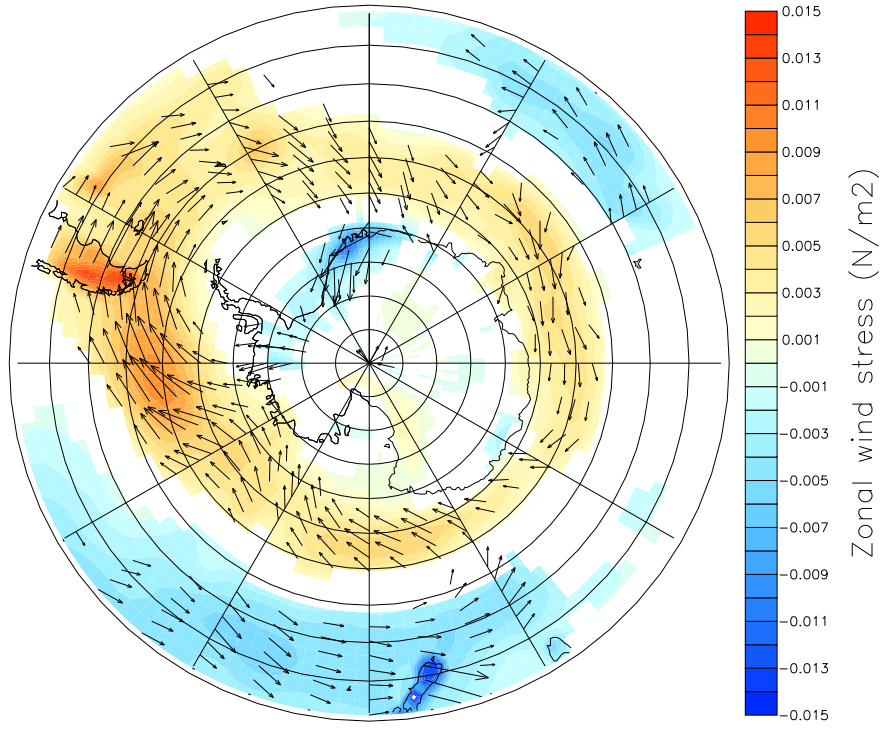

(b)

Figure 3.4: a Surface temperature anomalies (shading; °C) and sea level pressure (contours; hPa) anomalies for the warm phase (year 600-650) relative to the cold state (year 400-550). Contour lines are plotted in intervals corresponding to 0.1 hPa. b Zonal wind stress anomalies, τ_x (shading; N/m2) for the same period as in a. Vectors (N/m2) represents both zonal and meridional (τ_x and τ_y) components of the wind stress anomalies. Wind stress vectors are only plotted if anomalies are larger than 3×10^{-3}N/m2. Changes are only plotted if they are significant on 95% level, based on a t-test.

the observed increase in the air temperature in the Atlantic and Indian Ocean sectors of the Southern Ocean. The wind stress changes in figure 3.4b show intensification of the westerlies across the latitudes of the ACC associated with the anomalous cyclonic circulation. The changes are strongest in the Drake Passage and at the southern tip of South America, where the zonal wind-stress increase by up to 10% relatively to the cold state. However, the wind stress changes in the rest of the Southern Ocean in general are relatively small, which could also explain the weak response in surface temperatures. These results furthermore suggest that the atmospheric circulation changes in the southern high latitudes are weak compared to the Northern Hemisphere response. However, the observed circulation anomalies, inferred from figure 3.4a and 3.4b, exhibit some of the same characteristics associated with large scale modes of hemispheric climate variability such as the PSA pattern. This suggest a connection between tropical climate variability and changes in the climatic conditions in Antarctica. In the next section, we explore how the stochastic forcing, through the tropical-polar teleconnection, can trigger deep convection in the Weddell Sea, which provides a possible feedback mechanism in the Southern Hemisphere.

3.3 Deep convection in the Weddell Sea

3.3.1 General circulation in the Weddell Sea

The Weddell Sea is one of the primary regions of deep water formation in the Southern Ocean, where cold and high-salinity water, formed on the continental shelf, is mixed with warm deep water from the Weddell Gyre. The warm deep water (WDW) is a thick layer of relatively warm water, which is drawn from the Antarctic Circumpolar Current, cooling through mixing as it transits the gyre. Below the WDW are the Weddell Sea Deep Water (WSDW) and the Weddell Sea Bottom Water (WSBW), which both are cooled and freshened relatively to the WDW. The more saline, and thus heavier, WSBW is derived from the southwestern Weddell Sea, where high-salinity shelf water is abundant. The WSBW flows northwards, exiting the Weddell Sea at great depths, while mixing with the surrounding water masses to form AABW.

The formation of AABW is highly dependent on the high-salinity shelf water formed by brine release during sea ice formation along the coast of Antarctica. Here, strong katabatic winds continuously remove sea ice away from the coast, exposing the ocean to the cold polar atmosphere and inducing further sea ice formation. The high-salinity water produced on the shelf is mainly controlled by surface processes and is confined to the relatively shallow mixed layer. In the polar ocean, the mixed layer typically constitutes the upper 100-200 meters of the ocean and is largely dependent on the history of local surface wind stress and the stability of the underlying water [Pond and Pickard, 1983]. Hence, the maximum mixed layer depth, is largely determined by the magnitude of the surface wind stress, which provides a source of potential energy to mix the water, thereby weakening the stratification. However, if the surface layer is strongly stratified, mixing is weak and the mixed layer is shallow. This is the dominant situation in the Southern Ocean, where sea ice formation ensures a weakly stratified surface layer capping a thick layer of relatively warm saline deep water. However, if the surface layer becomes unstable, the mixing can reach all the way to the ocean floor, which is commonly known as deep convection events. This represents an alternative mode of Southern Ocean ventilation, where he primary production of bottom water is moved away from the continental shelf and into the deep regions of the Weddell Sea. This alternative mode of deep ocean ventilation is thought to play an important role in Southern Hemisphere climate through changes in deep ocean heat storage and modifying atmospheric CO_2 concentrations.

In this section, we will focus on some of the main features of bottom water formation in the Southern Ocean and explore the different processes that controls deep ocean ventilation in the CCSM4 simulation. Here, we concentrate on open-ocean deep convection in the Weddell Sea as a mechanism to ventilate the Southern Ocean and affect bottom water formation. Inspired by recent studies, we propose a mechanism which links the deep convection events in the Weddell Sea to stochastic climate variability in the tropics, thus providing a conceptual model for explaining the Antarctic temperature fluctuations during the last glacial.

3.3.2 Deep convection in the CCSM4 simulation

In the CCSM4 simulation we find, that deep convection events are a persistent feature of Southern Ocean climate variability, linked to a dynamical ocean-atmosphere coupling. During the convective phases deep convection is mainly observed in the Weddell Sea, where the mixed layer depth reaches the bottom of the ocean at 4,000 m depth. Smaller convective plumes are also found in the Ross Sea close to the continental shelf (not shown). This is illustrated in figure 3.5, which shows an example of the maximum boundary layer depth (BLD) and associated minimum sea ice concentrations in the Weddell Sea for a series of convective events (right) and a non-convective phase (left). What is particularly interesting about this relatively short period is that it coincide with the abrupt transition from a cold North Atlantic climate state into a warmer North Atlantic climate, described in section 3.1. As we point out in this section, the abrupt change in North Atlantic climate is triggered by a shift to a dominant La Niña state, is manifested as an increase in western tropical Pacific precipitation and an anomalous low centered over the Antarctic Peninsula and Weddell Sea.

The right panel in figure 3.5 shows the annual maximum boundary layer depth in a 3-year period from the integration years 591-593. This period is relatively unique in the sense that it is preceded by a long period without significantly deep convection in the Weddell Sea. The few years leading up to the convective phase is shown in the left panel of figure 3.5, and is characterized by an abrupt decrease in sea level pressure over the convective region. During the short convective phase the mixed boundary layer reaches a depth of 4,000 m, related to the vigorous mixing induced by the convective overturning. The convective region is confined to a relatively small area in the deep part of the Weddell Sea which we define as the Weddell Sea Convective Region (WSCR).

The areal extent of the convective event shown in figure 3.5 is about 150,000 km2. However, looking over the whole period of integration, we observe convective events that are up to 230,000 km2 in size, which matches quite well with observations [Gordon and Comiso, 1988]. This, however, suggests that there is a large variance in the spatial extent of the deep convection events throughout the simulation, which might be linked to changes in the atmospheric conditions over the Southern Ocean. The associated changes in sea ice concentration (white contour lines in figure 3.5) matches the spatial extent of the convective region, with the greatest decrease observed where deep convection occur. The sea ice concentration averaged over the WSCR decreases by 77% relatively to the non-convective phase. The contours also (of 75% sea ice concentration) reveals that the area of high sea ice concentration is highly affected by the deep convection event. This result agrees well with [Robertson et al., 2002], showing a large effect on melting of pack ice resulting from a warming trend in WDW due to absence of deep ocean ventilation.

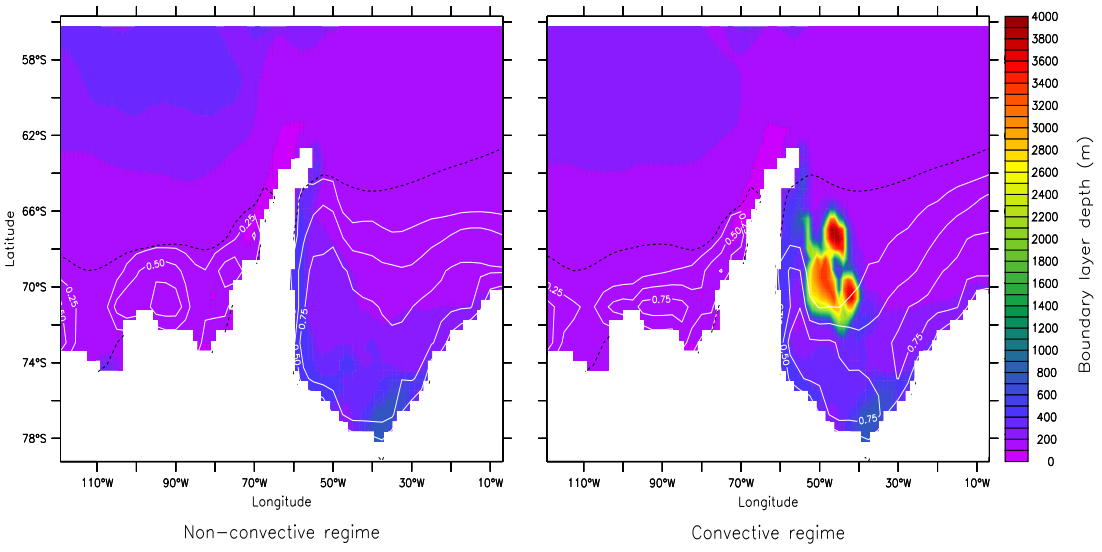

Figure 3.5: Annual maximum boundary layer depth [m] and 25%, 50% and 75% summmer sea ice concentration (white lines) during a non-convective (left) and a convective phase (right). The dashed black line represents the the long-term mean 25% summer sea ice concentration.

The left panel shows the maximum BLD for the three years leading up to the convective regime (i.e. integration years 587-590). Here, no open ocean convection is observed and the formation of cold and dense bottom water is confined to the shelf. Consequently, the annual minimum sea ice concentration is relatively high compared to the convective phase and is relatively close to the long-term mean (black dashed line). In absence of open ocean convection in the Weddell Sea, sea ice concentrations extends well beyond

$66°S$ east of the Peninsula. West of the Peninsula, minimum sea ice extent is relatively unchanged. However, there is a slight decrease in the maximum sea ice concentration during the non-convective phase, which could be related to anomalous on-shore winds in the Bellingshausen Sea leading to advection of sea ice towards the coast (decreasing sea ice concentration) [Ding et al., 2011].

Deep convection in the model is observed to occur at the end of the cooling season in September/October, when sea ice concentration reaches the annual maximum. This provides an important piece of information about the environmental forces leading to the deep convective events. The southwestern part of the Weddell Sea, where the main part of deep convection is observed, is characterized by a thin surface layer capping a thick layer of warm and salty bottom water separated by a weak pychnocline. During austral summer, the melting of sea ice ensures a weakly stratified surface layer of cold and fresh water. In winter, enhanced sea ice formation or strong cooling at the surface can cause a weakening of the stratification and lead to a breakdown of the stratification. This triggers deep convection with associated upwelling of warm and salty deep water. Figure 3.6 shows the water column characteristics for the non-convective (solid black lines) and convective phase (red dashed lines) and illustrate how deep convection can affect the stratification in the water column. The left (right) panel shows the annual potential temperature (salinity) averaged over the WSCR for the non-convective and the convective phase (e.g. same as in figure 3.5). During the pre-polynya state, the surface layer is relatively cold and fresh with ($\theta = -1.7°C$) and ($Sal = 34.37$). The thermocline sits at 100-200 m depth separating the surface mixed layer from a thick layer of relatively warm ($> 0°$C) and salty (> 34.70) deep water. This is the WDW, which is identified as a temperature maximum at $\approx$ 650m depth. The non-convective phase serves as a kind of pre-conditioning of the stratification within the Weddell Sea leading up to the deep convection event. During this pre-conditioning phase, the salinity in the upper 100 m is steadily increasing (by 3σ) from 34.37 to 34.46. This is related to sea ice production causing increased brine release, and a build-up of cold high-salinity water at the surface. In mid-winter, when the stratification is weakest, the surface layer becomes negatively buoyant and overturning of the water column leads to a deepening of the mixed layer. Significantly deep convective events can persist for several winters and is maintained by upwelling of warm deep water inhibiting sea ice production thus leading to anomalous low sea ice extent in summer, as shown in the right panel of figure 3.5. From figure 3.6 we observe a warming of the surface layer during episodes of deep convection

(corresponding to years 591-593), where WDW of $\theta \approx 0.7°C$) is brought to the surface leading to increased SST's and subsequent sea ice melt in the convective region. In turn, the WDW has cooled by $\approx 0.3°C$ due to the downwelling of cold surface water. The salinity also increases in the upper 100 m, which suggest a positive flux of salt out of the deep layer and into the surface layer associated with the convective overturning. This leads to a shallower thermocline and pychnocline which further reduces the stability of the water column. Towards the end of the deep convection phase, the surface salinity decreases and the pychnocline strengthen increasing the stability thus inhibiting deep convection. The biggest changes are primarily confined to the top 1000 meters, with relatively modest changes in the deep ocean. There is only a small cooling of the WSDW associated with the deep convection, which imply that the deep convection observed in the CCSM4 simulation has little impact on the WSBW and deep-ocean heat storage.

The weak stratification observed in the Weddell Sea illustrates, that the WSCR is very sensitive to small density variations at the surface. This is consistent with a number of studies of Southern Ocean ventilation, which has been given much attention recently [de Lavergne et al., 2014, Gordon et al., 2007, McKee et al., 2011]. In the following analysis, we include some these studies along with observations from the Weddell Sea, and explore the potential sensitivity of Southern Ocean deep convection to changes in local atmospheric circulation. We focus on the relationship between the atmospheric conditions, which is the controlling factor on the stratification in the Weddell Sea, and open-ocean deep convection observed in the CCSM4 integration.

3.3.3 Sensitivity of Southern Ocean deep convection

Figure 3.7a shows the time series of the annual maximum boundary layer depth in the WSCR and illustrates the occurrences of multiple deep convection events throughout the model integration. The average depth of the mixed layer, during non-convective events is between 100-200 meters. However, during deep convection events the mixed layer deepens significantly reaching all the way to the ocean floor. Here, we define significant deep convection as a boundary layer depth of $> 2,000$ m. This value is chosen to make sure that we only capture the open-ocean deep convection and not the dominant mode of deep ocean ventilation that occur on the shelf and continental slopes. By restricting boundary layer depth to $> 2,000$ m we also ensure that the deep convection penetrates

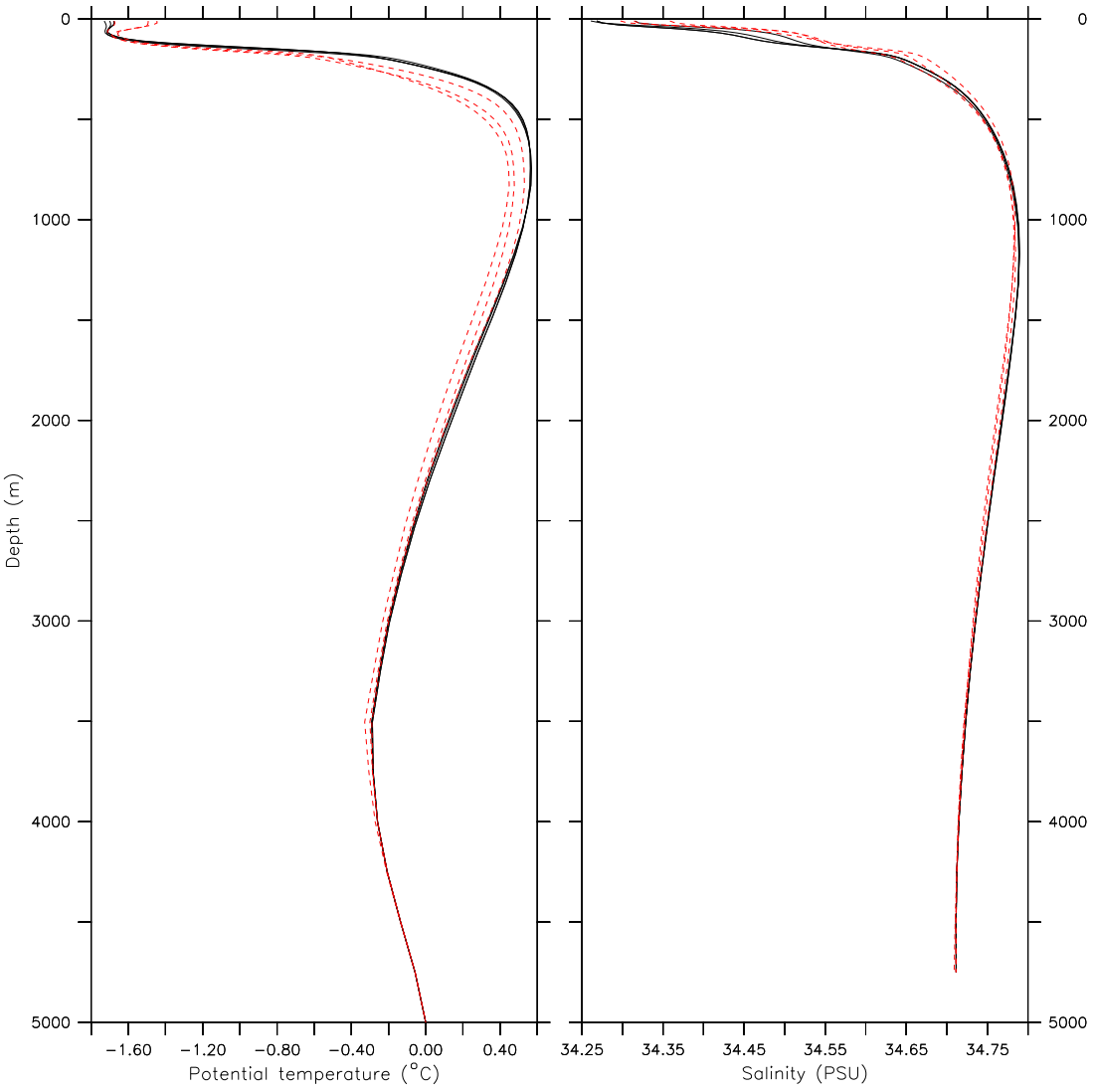

Figure 3.6: Profiles of potential temperature $[\theta°C]$ and salinity $[g/kg]$ in the Weddell Sea Convective Region. Solid black lines; before the convective event, red dashed lines; during deep convection event.

the warm and salty deep water which is essential to form the open-ocean polynyas, that we observe in the model. Furthermore, this is the same depth chosen by [de Lavergne et al., 2014], which enables a meaningful comparison. The upwelling of warm deep water associated with the deep reaching overturning is a key component in maintaining ventilation of the deep ocean by facilitating a direct pathway between the surface and the deep ocean. This could potentially affect global climate on longer time scales due to the effect on AABW following the idea by [Broecker, 1998]. We find that $\approx$ 17% of all model years exhibit deep convection, reflecting that Southern Ocean ventilation happened relatively frequent under pre-industrial conditions.This value is significantly

lower than the 63% reported by [de Lavergne et al., 2014]. Figure 3.7b shows the spread of the duration of convective events in the CCSM4 simulation and the spacing between events (i.e. duration of the non-convective phases). The mean duration of convective events is 1.6 years, with a mean spacing between events of about 8 year. Though, the duration of convection in the model appears to change significantly throughout the integration and the mean spacing between events also varies notably. In the first 200-300 years of the model integration, convection happens more frequently with durations of up to 10 years. Towards the end of the integration, convection becomes more intermittent and generally only persists for a few years.

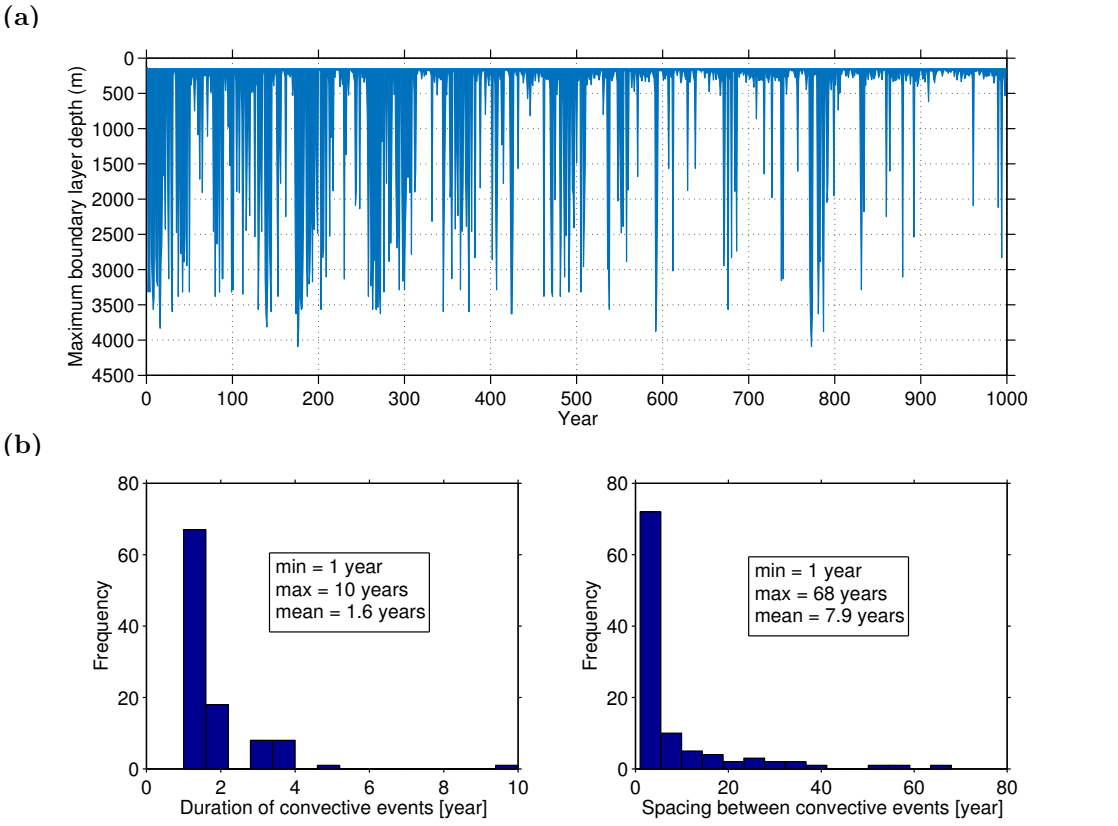

Figure 3.7: a Annual maximum boundary layer depth (m) in the convective region of the Weddell Sea ($64° - 72°S, 36° - 50°W$).b Simple statistics of the deep convection events showing duration and mean spacing between convective events.

The upper panel in figure 3.8 shows the areal extent of significant deep convection in the Weddell Sea expressed as the normalized convection area. By looking at the convective area rather than just the maximum boundary layer depth, we can compare the relative strength of the different events and their impact on sea ice and sea surface temperatures. By comparing to figure 3.7a we see that many of the deep-reaching events ($> 2,000$ m) are relatively small in extent, which indicates that a large part of the open-ocean deep

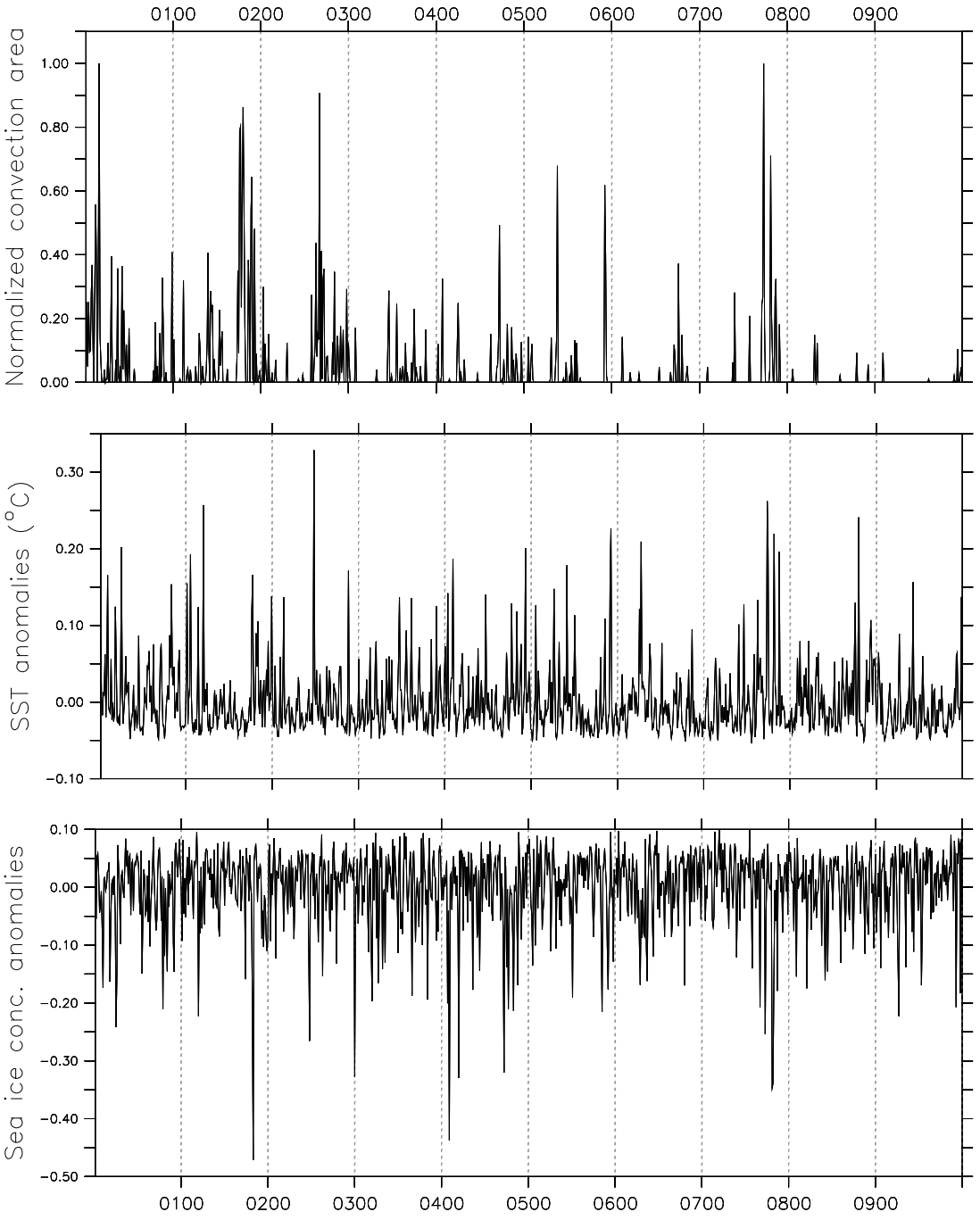

Figure 3.8: *Top* Normalized convective area for significant deep ($> 2,000m$) convection. For each event the convective area is normalized by the maximum areal extent recorded in the entire simulation.*Middle* Sea surface temperature anomalies ($°C$) relatively to the long-term mean averaged over the WSCR.*Bottom* Maximum sea ice concentration anomalies in the WSCR.

convection in the model is confined to smaller convective plumes. We imagine, that the extent of the convection area, is most likely the dominating factor in driving changes in sea ice and subsequent ocean-atmosphere heat fluxes. Here, we also observe a decreasing trend in the strength of deep convection with a series of strong and long-lived convective events during the first 300 years of the integration. The relatively big event towards the end of the integration is coinciding with the transition into the 2nd cold phase (see figure 3.1). We note, however, that there is no consistent pattern between cold and warm phases of North Atlantic climate and deep convection in the Southern Ocean. Hence, deep convection occur in both warm and cold phases and appears to be far more stochastic in nature, which is consistent with our previously proposed teleconnection mechanism. In general, we find that the strong and big convective events are associated with significant decrease in sea ice and increase in SST's in WSCR. The convection primarily occur in a region of the Weddell Sea mostly covered by perennial sea ice (i.e. multi-year ice). This has a strong effect on the maximum sea ice concentration which decreases by up to 50% during episodes of deep convection (lower panel of figure 3.8). The amount of heat, being brought to the surface from deeper and warmer layers, is large enough to melt away the thick pack ice, and increase the sea surface temperature over that region. This abrupt surface warming coincide with some of the bigger deep convection events (middle panel in figure 3.8) and points to the fact that convective overturning is a key aspect explaining the melting of the pack ice.
However, the abrupt changes in sea ice concentration and SST's does not always match up with the larger deep convection events and suggest that even some of the small and short-lived convective events can impact the surface quite significantly. Moreover, the deep convective events cannot solely explain the variability in sea ice concentration and SST over the convective region. Here, the stochastic forcing by the atmosphere has an important role in modulating sea ice formation and also driving the variance in SST's.

The intermittent nature of the deep convection events illustrated in figure 3.8 presents an important clue about the triggering mechanism. By looking at the timing of the largest convective events in the Weddell Sea relatively to the sea level pressure anomalies in figure 3.3a, we find that the open ocean convection is closely linked to the abrupt changes in atmospheric circulation over the Weddell Sea region. These abrupt changes are expressed through an atmospheric teleconnection mechanism between the tropical Pacific and the Southern Ocean. Hence, we argue that the large variability in the deep

convection and sea ice concentration in the Weddell Sea is inherited from the stochastic variability of the tropical forcing.

3.4 Ocean circulation response to North Atlantic cooling

In the previous chapter we focused on the atmospheric teleconnection between the tropical Pacific and high latitude climate and the possibility that stochastic climate variability, triggered by tropical precipitation anomalies, can influence Southern Hemisphere climate on centennial time scales. In this section, however, we return to the classic view on the coupling between northern and southern hemisphere climate, and turn our focus towards the changes observed in the Atlantic ocean circulation related to the abrupt climate transitions in the North Atlantic. Here, we examine the adjustment of the ocean circulation in the Atlantic in the first couple of decades after the abrupt transition in North Atlantic climate.

The following analysis is split in two primary subsections, in which we focus on different ways that changes in ocean circulation can trigger transitions in Southern Hemisphere climate. The first part is motivated by a number of recent studies that focus on how cooling in the North Atlantic and corresponding AMOC slowdown, can trigger an atmosphere-ocean teleconnection which explains the asymmetric nature of the north-south coupling [Chiang et al., 2008, Lee et al., 2011]. For the second part, we go back to the classic idea of a bipolar see-saw driven by changes in the Atlantic meridional overturning circulation that are communicated to the Southern Hemisphere through an oceanic bridge [Broecker, 1998, Crowley, 1992, Stocker and Thomas, 1998]. We focus our analysis on ocean dynamics and signal propagation in the Atlantic Ocean based on the current theoretical understanding of the abyssal circulation described in [Stommel and Arons, 1959–1960] and [Kawase, 1987].

3.4.1 Subsurface warming in the North Atlantic

Figure 3.9 shows a cross section of the Atlantic Ocean with the zonally averaged annual potential temperature anomalies associated with the cooling event in the North Atlantic. Hence, the anomalies show the difference in potential temperature between the first cold

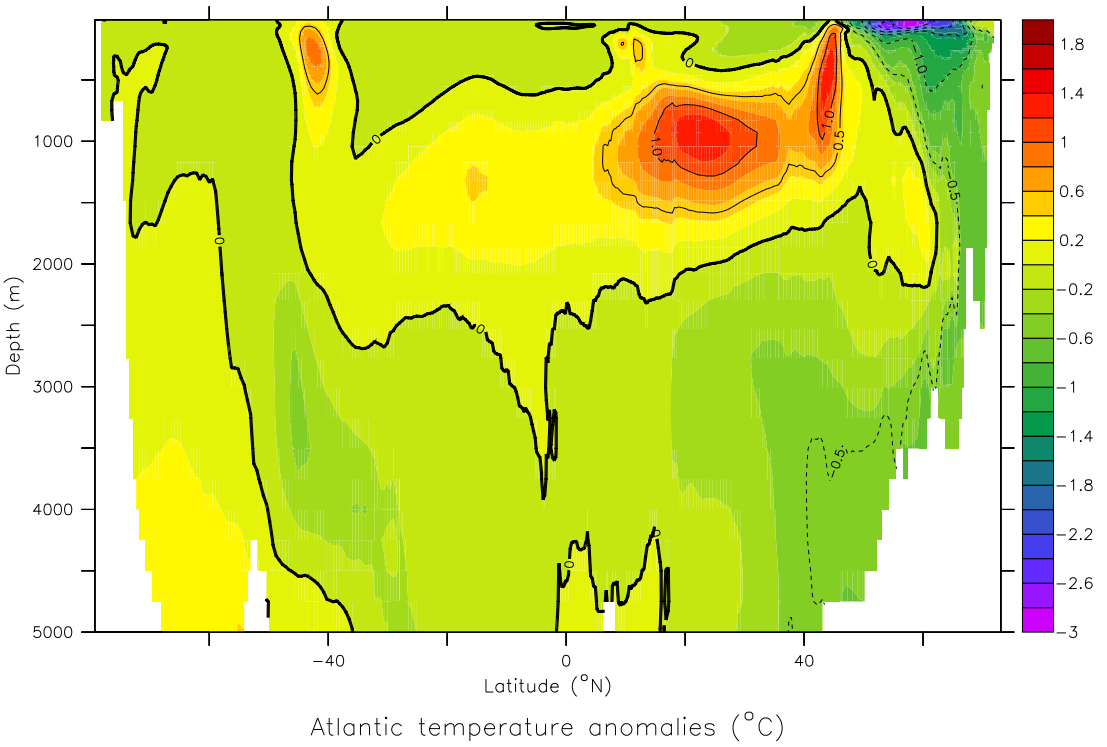

Figure 3.9: Depth-latitude cross section of the Atlantic Ocean showing potential temperature anomalies (cold-warm phase). Anomalies are zonally averaged over the Atlantic basin.

NA phase (year 400-550) and the warm phase (year 50-250), described in section 3.1. In the northern high latitudes we observe a relatively strong cooling of $1 - 3°C$ in the upper 1000 m of the ocean. The temperature response is strongest in the surface in the Labrador Sea (about $5 - 6°C$ at the core). In the northern midlatitudes, there is an intense surface warming located at about 42°N, which roughly represents the boundary between the subpolar gyre and the subtropical gyre. This illustrates a strong dipole pattern in the North Atlantic surface ocean with a very localized warming at the subpolar-subtropical gyre boundary and widespread cooling north of it. This suggests an essential role for the gyre circulation to transport heat into high latitudes. [Kleppin et al., 2015] associates the surface cooling in the North Atlantic with a weakening of the subpolar gyre circulation caused by a reduction in the wind stress from a persistent atmospheric circulation anomaly and consequently a weakened ocean-atmosphere heat flux in this region. To illustrate this point, we plot the surface ocean temperature anomalies along with the barotropic streamfunction in figure 3.10.[1] Here, the dipole

[1]The barotropic streamfunction is the zonally integrated mass transport associated with the surface wind-stress. Positive (negative) values corresponds to anticyclonic (cyclonic) circulation. Hence, the mean subpolar gyre circulation is cyclonic i.e. streamfunction is negative whereas the subtropical gyre is characterized by anticyclonic circulation with a positive streamfunction.

pattern is evident as a widespread cooling in the subpolar gyre region and an intense warming just off the east coast of North America around 40°S. We find, that the extend of the cold anomaly in the surface ocean, matches with the circulation changes in the SPG region. The barotropic streamfunction (contours), shows a significant weakening of the subpolar gyre circulation by 30% [Kleppin et al., 2015] relative to the mean state, and causes an increase in sea ice cover in the Labrador Sea.

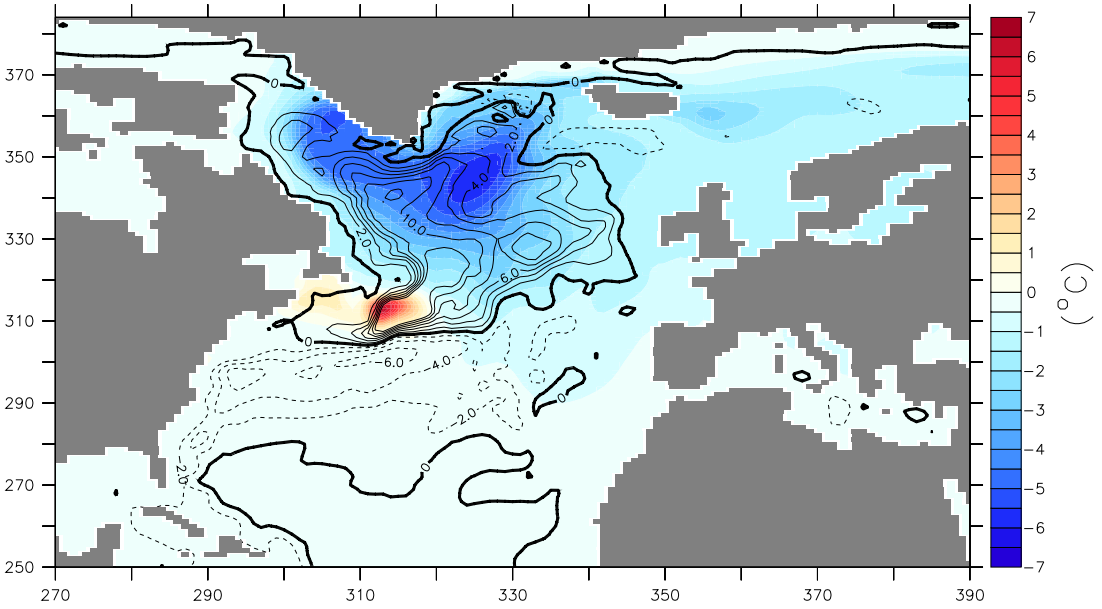

Figure 3.10: Anomalies of potential temperature (*shading*;° C) in the surface ocean (upper 5 meters) and barotropic streamfunction (*contours*; Sv). The anomalies are calculated taking years 400-550 corresponding to the North Atlantic cold phase and using years 50-250 (warm phase) as a base.

The cooling of the northern high latitudes is further aided by a weak reduction in the subtropical gyre circulation, which reduces the northward advection of warm saline water. This is depicted as a negative (i.e. cyclonic) anomaly in the barotropic streamfunction in the North Atlantic midlatitudes. Consequently, we observe a build up of heat at the subpolar-subtropical gyre boundary due to the reduced northward ocean heat transport into the northern North Atlantic. Hence, the primary mechanism behind the widespread surface cooling in the Northern Hemispshere high latitudes is the reduced advection of warm and saline subtropical water to high latitudes associated with the weakened gyre circulation leading to a persistent weak state of the SPG circulation.The circulation in the subpolar gyre is driven by the strong prevailing westerlies, creating a southward Ekman transport. The westerlies decrease in magnitude going southward, leading to Ekman divergence and subsequent upwelling due to *Ekman pumping*. In the

North Atlantic midlatitudes the easterlies drive a northward Ekman flow driving the subtropical gyre. At the boundary between the subtropical and subpolar gyre the Ekman flow goes to zero due to convergence of the winds. Hence, this region there will be a convergence of the horizontal flow and downwelling. From figure 3.9 we see that the intense surface warming at the subpolar front is mediated to mid-depths, which is consistent with the Ekman induced downwelling at the intergyre boundary. The subsurface warming spreads southwards through the Atlantic Ocean confined to a relatively well-defined depth interval between 500-1500 m, corresponding to the lower boundary of the wind-driven surface layer. The warming signal is strongest (about 2°C) in the North Atlantic midlatitudes and weakens as the signal propagates into the South Atlantic.

3.4.2 Changes in AMOC

The slowdown of the AMOC is depicted in figure 3.11, showing a cross section of the Atlantic Ocean, where the anomalies (*shading*) corresponds to the same period as in figure 3.9. The overturning circulation changes resembles the pattern of the anomalous temperatures in the Atlantic Ocean with the largest weakening of about $6Sv$ at 40°S between 1000 and 2000 m depth. This matches quite well with the previous notion, that the mid-depth warming in the midlatitude North Atlantic is associated with a weakening of the AMOC and subsequent heat convergence near the subpolar front. In the rest of the Atlantic there is a relatively small reduction in the AMOC.

The time series of the maximum overturning circulation in the North and South Atlantic (3.11 - *top panel*) shows the AMOC variability throughout the model integration. Here, the maximum overturning is defined between 1000-3000 m depth, where the black and red line corresponds to the North Atlantic at 40°N and the South Atlantic at 20°S respectively. The transition into the cold phase is characterized by a gradual weakening of 3-4 Sv, with a similar pattern observed in the Southern Hemisphere (*red curve;* $20°S$). However, the AMOC changes are significantly weaker and lags the Northern Hemisphere by about 16 years. This time-lag suggest a slow ocean adjustment to the climate transition in the North Atlantic, which is in contrast to the fast atmospheric teleconnection described in the previous section. Towards the end of the cold phase, an abrupt resumption of the AMOC is associated with the abrupt sea ice retreat in the Labrador Sea thus enabling a more active deep water formation at the transition into

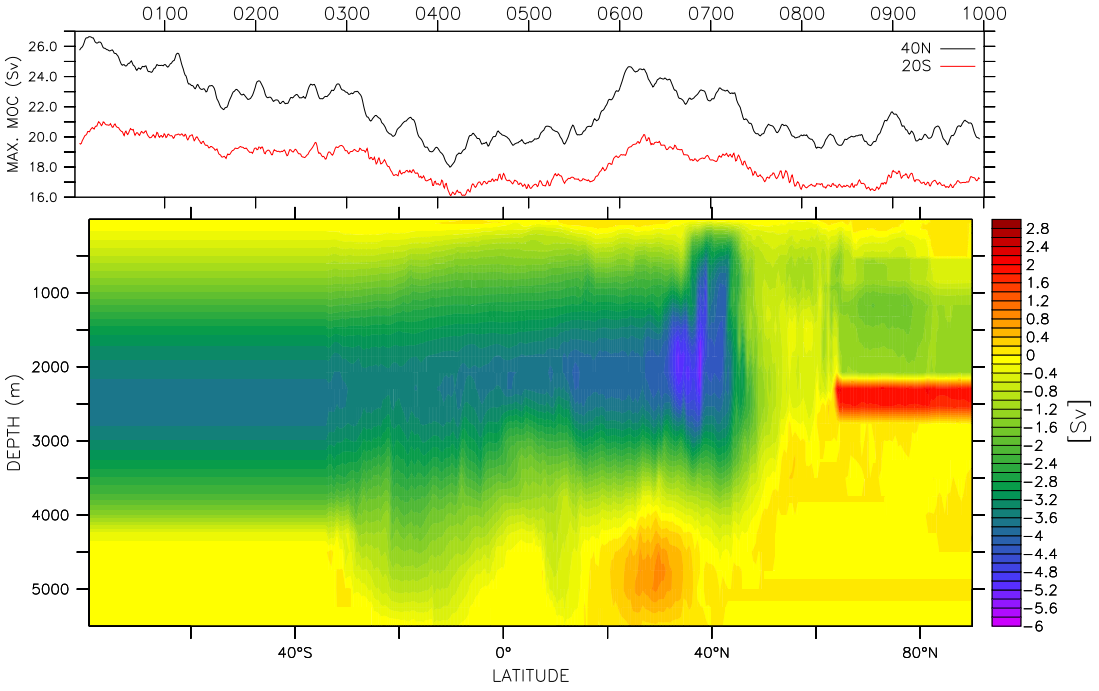

Figure 3.11: Changes in the Atlantic meridonal overturning circulation (AMOC). *Top* Time series of the maximum AMOC (Sv) between 1000-3000 m depth for the North Atlantic (40°N; *black*) and the South Atlantic (20°S; *red*). Both time series are smoothed with a running mean of 10 years. *Bottom* Difference in AMOC strength (Sv) between the NA cold phase (year 400-550) and the NA warm phase (year 50-250) for the Atlantic basin.

the 2nd NA warm phase (around year 600). This again leads to an increased advection of warm subtropical water into the high latitude North Atlantic.

3.4.3 Atmosphere-ocean teleconnection – Chiang hypothesis

In this section we analyze the subsequent equatorwards progression of the mid-depth warming in the Atlantic with reference to previously mentioned atmosphere-surface ocean teleconnection described in [Chiang et al., 2008]. The results presented in the previous section show a warming anomaly in the Atlantic spreading southward at mid-depth. The warming is strongest in the North Atlantic midlatitudes and gradually weakens as the it spreads through the basin and into the South Atlantic. However, south of the equator, at about 20°S, we find a small positive anomaly at 1500 m depth which appear to be detached from the warming signal in the Northern Hemisphere. Hence, the warming anomly appears to be stronger in the midlatitude South Atlantic compared to the response in the tropical South Atlantic. This would indicate a teleconnection mechanism which could amplify the signal in the midlatitudes through an

ocean-atmosphere feedback mechanism. The warming signal spreads further throughout the South Atlantic, where it appear to stagnate at about 30°S. South of this point, the warm anomaly exhibits a structure associated with an upwelling from mid-depth into the surface layer, where a relatively strong surface warming centered between 40°S and 45°. This region corresponds to the boundary between the South Atlantic Gyre (SAG) and the Antarctic Circumpolar Current (ACC), which is dominated by the strong prevailing westerly winds. Hence, our initial thought was that the surface warming was related to changes in the zonal wind-stress driving increased upwelling, similar to the mechanism described in [Lee et al., 2011] and [Chiang et al., 2008]. An essential part of the teleconnection mechanism, originally proposed by [Chiang and Bitz, 2005], is the pronounced southward displacement of the tropical Atlantic ITCZ which is a robust climate response to the slowdown of the AMOC. When the Northern Hemisphere cools the Atlantic ITCZ moves southwards (i.e. towards the warmer hemisphere). The southward shift in the ITCZ causes changes in the Hadley circulation, with a weakening of the southern Hadley cell and a reduction of the Southern Hemisphere subtropical jet. This can be observed as a southward shift in precipitation due to displacement of the region of maximum vertical velocity. To counterbalance the weakened subtropical jet, there is an increase in the eddy-driven SH midlatitude westerlies, which causes increased wind-driven upwelling in the Southern Ocean (see figure A.3).

In the CCSM4 simulation we find a similar pattern in the wind-stress and precipitation anomalies in the tropical Atlantic associated with the North Atlantic cooling (figure A.1). There is a small intensification of the northeasterly trade winds, which seems to be a general feature of tropical Atlantic response to the southward shift of the Atlantic ITCZ, inferred from GCM simulations [Chiang et al., 2008, Lee et al., 2011, Timmermann et al., 2010]. A southward shift in the tropical Atlantic precipitation is observed associated with the North Atlantic cooling, however the changes are significantly smaller compared to the changes observed by [Lee et al., 2011]. Hence, the associated wind-stress changes are also weak and does not seem to explain the warm anomaly in the surface ocean at 40°S. We find, however, that a large part of the observed variability is most likely associated with a model drift in the first 200 years of the simulation. This can be explained by the initial spin-up from observations, which causes a slow adjustment of the surface ocean.

3.4.4 Spatial structure and propagation of the subsurface warming

Here we go back to the original bipolar see-saw idea motivated by the subsurface warming signal spreading through the Atlantic Ocean. In this section we explore, how the current theoretical understanding of the general ocean circulation can help us understand the spatial extent and signal propagation of the mid-depth warming anomaly in the Atlantic.

In the previous section, we showed that the largest changes in both AMOC and temperature are confined to a depth of about 1,000 m in the Atlantic Ocean. Hence, figure 3.12 shows the evolution of a warming anomaly in 1,000 m depth starting at the onset of the abrupt climate transition in the North Atlantic. Here we show snapshots of 10 year intervals of the potential temperature anomalies in the 1,000 m depth layer. The anomalies are calculated using the long-term-mean, which is computed for each grid point in the Atlantic basin.

Initially (year 320), there is a widespread cold anomaly in the Northern Hemisphere extending from the subtropics to the midlatitudes at 40°S. This pattern of the anomalously cold temperatures correspond quite well with the mean circulation of the wind-driven subtropical gyre. At the onset of the NA climate transition, an anticyclonic sea level pressure anomaly evolves over the northern North Atlantic and moves westward into the subpolar gyre region. The atmospheric changes over the subpolar gyre provides a near-instantaneous response in the gyre circulation through changes in the wind-stress curl. However, the subsequent adjustment in the ocean heat content is somewhat slower. Our previous analysis suggests that this time scale is set by the gradual weakening of the AMOC, thus slowly reducing the northward ocean heat transport. This is illustrated as a gradual decrease in the extent of the cold anomaly in the northern midlatitudes during the initial ocean adjustment to the atmospheric circulation changes in the subpolar gyre region (years 320-350). This is countered by a slowly evolving warming anomaly at the boundary between the subpolar and subtropical gyre related to the reduced advection of warm water by the weakened gyre circulation.

Around year 350 a consistent positive anomaly evolves around 40°N just south of New Foundland and is slowly replacing the anomalous cold temperatures in the subtropical gyre. At year 390 the warming is fully developed and covers most of the North Atlantic midlatitudes. The spreading of the temperature anomaly is consistent with the anticyclonic circulation in the subtropical gyre with an eastward flow into the interior in the

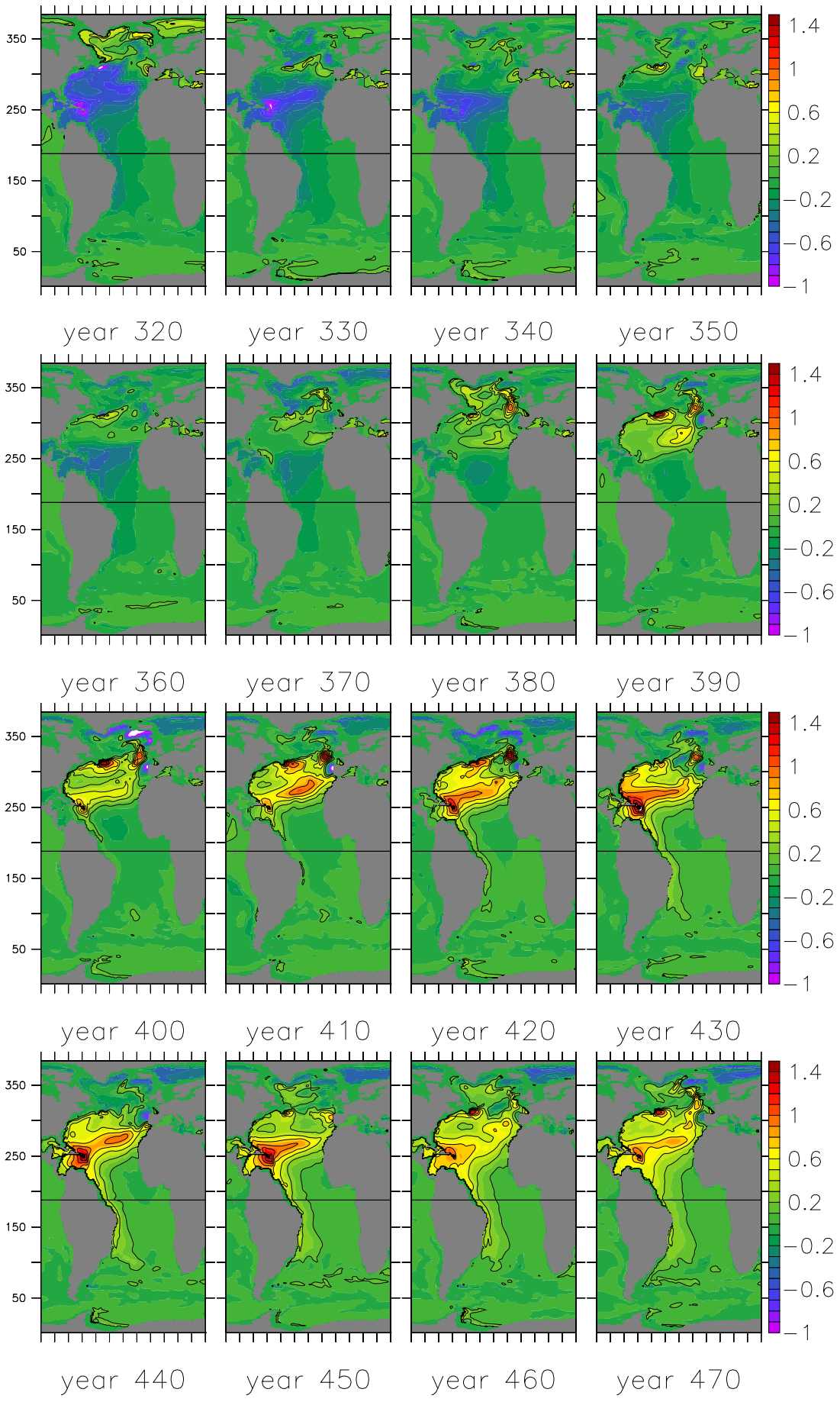

Figure 3.12: Contour lines are only plotted if the anomaly is larger than 0.1°C with an interval of 0.2°C. The axes correspond to grid point longitudes and latitudes, where the solid line represents the equator and the values 115 and 304 corresponds to 20°S and 40°N respectively.

northern part of the gyre and a westward return-flow to the south. In the northern part of the subtropical gyre, we observe a tongue of warm deep water spreading towards the Nordic Seas following the northeastward path of the North Atlantic Drift.

From year 390 and onwards the mid-depth warming continues to spread throughout the Atlantic, however now the signal propagation seems to be confined to the western boundary. Here, a thin and well-constrained tongue of anomalous warm water is emanating from the subtropical gyre spreading along the western boundary. Around year 420 the warming signal has reached equator and spreads into the tropical South Atlantic. In the tropical South Atlantic, the spreading rate appears to be significantly faster and within 10 years the signal has traveled from the equator to 20°S. It takes another couple of decades for the signal to reach 40°S corresponding to the southernmost boundary of the South Atlantic Gyre, where it cannot propagate further southwards. Due to its strong baroclinic structure, the ACC acts as a barrier against meridional flow thus limiting the poleward heat transport. Hence, at the northern boundary of the Southern Ocean, the warm anomaly is spreading eastward with the mean gyre circulation influenced by the strong eastward-flow of the South Atlantic gyre. By the time the signal reaches the subtropical South Atlantic the temperature anomaly has decreased by about 70% (from 1.5°C to 0.4°C) relative to the initial anomaly in the North Atlantic. South of the ACC, there is no longer any trace of the warming signal.

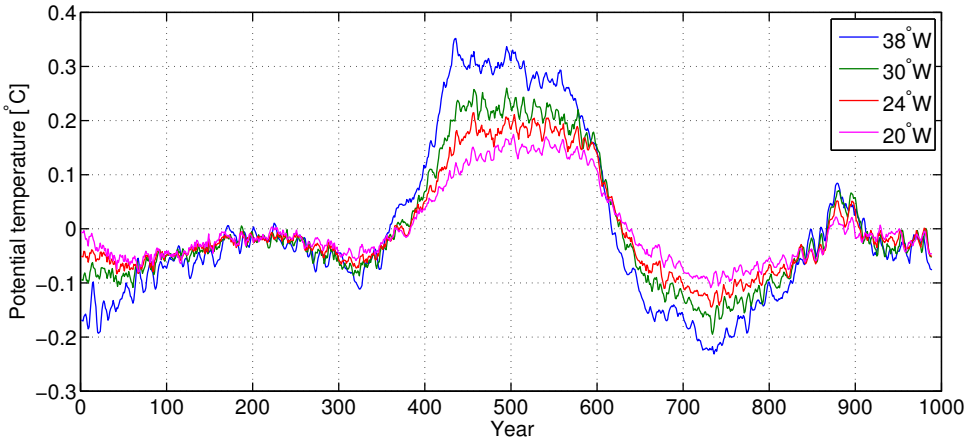

Figure 3.13: Potential temperature anomalies (°C) in 1000 m depth at 20°S. Line colors corresponds to different longitudes with increasing distance from the western boundary; *blue*; $^{3}8\circ$W, *green*; $^{3}0\circ$W, *red*; $^{2}4\circ$W and *magenta*; $^{2}0\circ$W.

From figure 3.12 it is clear that the western boundary plays an essential role in the

southward propagation of the temperature signal. The signal is strongest close to the western boundary and tappers off as we move eastward into the interior. This is illustrated in figure 3.13, which shows the potential temperature at 1,000 m depth and for different longitudes in the South Atlantic at 20°S. The signal has been detrended using a simple linear fit and we applied a 10 year running mean to remove inter-annual variability. Here, we find that the amplitude of the temperature signal decreases with increasing distance from the western boundary.

3.4.5 Propagation through the deep western boundary current

In this section we give a brief introduction to the theoretical basis for the abyssal circulation, which we include in our discussion of the signal propagation in the Atlantic and the time-scales involved. Here, we discuss the two main processes of signal propagation in the Atlantic through the oceanic bridge; advection represented by the classic paper by Stommel and Arons ([Stommel and Arons, 1959–1960]) and wave adjustment processes described in [Kawase, 1987]. In view of these separate mechanisms, we analyze the southward propagation of the warm anomaly in the Atlantic Ocean depicted in figure 3.12. Here, we focus primarily on the ocean dynamics behind the signal propagation in the ocean as well as the time-scales associated with them.

3.4.5.1 Stommel and Arons

In a series of papers from 1958-1960, Henry Stommel and Arnold Arons laid the foundation of our present understanding of the abyssal circulation based on fundamental ideas about the state of the ocean [Stommel and Arons, 1959–1960].
The ocean is represented as a simple 2-layer model with localized sinking at high latitudes and western boundary currents are added to satisfy mass conservation. Here, the upper and lower layer represents the thermocline, driven by the wind and the abyss respectively. There is a flow from the upper layer to the abyss simulating sinking of cold and dense water associated with deep convection, which provides the driving mechanism for the interior flow. The distributed sinking is counteracted by a return flow in the interior from the lower layer to the upper layer. Here, a uniform upwelling with vertical velocity w_0 is assumed everywhere in the interior based on the idea by Munk (*Abyssal Recipies, 1966*). Thus, the vertical flow is meant to represent the upward advection

of heat from the abyss, which is inferred from a balance between the diffusion and the vertical advection of temperature. Following some of the earlier ideas by Stommel, the motion of the abyss is geostrophic and the interior solution is in geostrophic Sverdrup balance. Hence, from this it follows that as long as the vertical velocity w_0 is positive, corresponding to upwelling into the thermocline, the meridional velocity is always poleward. Hence, in the Southern Hemisphere the interior flow is to the south and to the north in the Northern Hemisphere. This surprising result is some what counter-intuitive because it means that the interior flow is always towards the sinking source. Furthermore, as a consequence there is a divergence at the equator, implying that there cannot be an interior flow across the equator. In order to close the circulation, western boundary currents are added in need to satisfy mass conservation. At the western boundary the geostrophic Sverdrup balance is upset, which allows for a cross equatorial flow and shows an illuminating result of the dynamics of the abyssal circulation.

To understand the structure of the abyssal circulation in the Stommel-Arons theory it is useful to think in terms of potential vorticity conservation. The potential vorticity $((\zeta + f)/D)$ relates the oscillatory motions associated with variation in the Coriolis parameter and the stretching and squeezing of a water column, where D is the layer thickness, ζ the relative vorticity and f is the Coriolis parameter. In the mid-ocean the horizontal shear is negligible (i.e. $\zeta \approx 0$). Thus, if D increases there must be a poleward flow leading to an increase in f while ζ remains small. Hence, conservation of potential vorticity leads to a poleward flow everywhere in the interior. The upward motion everywhere in the interior induced by the uniform upwelling into the thermocline causes the thickness D to increase, which results in a poleward flow in the Northern and Southern Hemisphere. To counterbalance the poleward interior flow, there must be a southward (northward) flow in the Northern Hemisphere (Southern Hemisphere). In the Northern Hemisphere this requires an input of negative vorticity due to the southward flow (i.e. decreasing f). This can be obtained by friction associated with the strong flow and horizontal shear at the western boundary. The combination of southward flow and strong shear on the western boundary induce an input of negative vorticity (anticyclonic motion) in the Northern Hemisphere. This further implies that a southward flow can only be sustained at the western boundary, which consequently leads to a deep western boundary current extending southwards from the source region in the Northern Hemisphere and across the equator to the Southern Hemisphere.

Hence, from these relative simple considerations Stommel and Arons showed the existence of a equatorward return-flow confined to the western boundary beneath the wind-driven surface layer. The key idea is the uniform upwelling as a direct response to the motion of the thermocline driven by mechanical- (i.e. wind) and buoyancy-forcing. This leads to a conceptual model of the abyssal circulation, with a geostrophically balanced and poleward flow everywhere in the interior and a return flow by the deep western boundary current.

3.4.5.2 Kawase

The structure of the abyssal flow inferred from the Stommel-Arons model is based on the key assumption that the distribution of the upwelling is completely independent on the motion of the abyss. However, observations of the abyssal flow show a strong baroclinic structure of the deep circulation, which is not represented in the Stommel-Arons model. Hence, extending the ideas of the Stommel and Arons model, [Kawase, 1987] presented an alternative view on the abyssal circulation by taking into account the baroclinic nature of the deep ocean.

Where Stommel and Arons relates the structure of the abyssal circulation to a widespread upwelling into the thermocline, Kawase assumed that the upwelling into the thermocline depends only on the motion of the abyss itself. This means that the abyssal flow is independent of the thermocline and the flow is strictly baroclinic in Kawase's model. Hence, the structure of the interior flow is dominated by the internal abyssal dynamics and controlled by baroclinic wave processes. The key assumption in Kawase's contribution is that the vertical velocity (i.e. upwelling from the deep layer) is time-dependent and consequently showed that propagation of Kelvin and Rossby waves plays a central role in setting up the structure of the interior flow. To understand the effect of the baroclinic wave response, we consider the evolution of a flow-field driven by an initial trigger in the northwestern side of the basin. This is somewhat consistent with the warm anomaly located on the western side of the North Atlantic basin (see figure 3.10). This initial perturbation induce a coastal Kelvin wave that propagates southward along the western boundary. Here, the lateral boundaries provide a source to sustain a zonal pressure gradient where the amplitude is greatest at the boundary and decays exponentially away from it. From geostrophy, the Kelvin wave has to propagate forward with the boundary on the right in the Northern Hemisphere and to the left in the Southern Hemisphere.

Upon reaching the equator the Kelvin wave is forced to move eastward, since the Kelvin wave cannot cross the equator on the western boundary due to the change in sign of f. Here, the equatorial zone essentially acts as a waveguide, providing a lateral boundary for the Kelvin wave which propagates from west to east without dispersion. The equatorial confined deep flow is associated with this eastward wave-propagation in the equatorial waveguide and is an essential feature of the equatorial ocean circulation, that the Stommel and Arons model failed to explain. When this equatorial Kelvin wave reaches the eastern boundary it splits and propagates polewards in both hemispheres. At the eastern boundary the pressure gradient cannot be fully sustained, and the eastern boundary is "leaky" and radiates Rossby waves into the interior.

Rossby waves are large-scale oscillatory motions associated with variations in the Coriolis parameter with latitude (i.e. the $\beta - effect$), so as the Kelvin wave propagates polewards (increasing f), Rossby waves are emmanating from the eastern boundary. One of the primary characteristics of the Rossby wave, is that the phase velocity always has a westward component. Hence, the signal is propagating westward away from the eastern boundary and fills up the interior which means that the structure of the interior flow is determined by the Rossby wave propagation.

The general structure of the abyssal flow is somewhat similar to the Stommel-Arons model, though the dynamics are qualitatively different. However, both models suggest that the deep western boundary current is an essential part of the deep circulation and provides a communication pathway between high and low latitudes. The flow described by [Kawase, 1987], provides a fast response mechanism to convey a localized perturbation through the Atlantic Ocean and across the equator through Kelvin and Rossby waves. This wave adjustment response is much faster than advective processes inferred from the advective processes described in the Stommel-Arons model.

The spatial pattern of the signal propagation showed in figure 3.12 is consistent with the dynamical framework of the deep ocean circulation portrayed by Stommel and Arons. In particular, the southward propagation of the temperature anomaly is a striking example of the deep western boundary current and it clearly shows the significance of the western boundary as an oceanic brigde connecting the Northern and Southern Hemisphere. This is illustrated as a strong zonal difference in the magnitude of the warming anomaly as it propagates southward. In the northern Atlantic midlatitudes the timescale and magnitude of the warming at mid-depth is set by the subtropical gyre circulation, and the heat convergence at the intergyre boundary. The warm temperature anomaly is carried

with the gyre circulation, steadily decreasing as it propagates southwards. This is illustrated in figure 3.14, which shows the time series of the warming anomaly at different latitudes in the Atlantic. The different locations, denoted by circles in the lower left panel, are chosen such that they are located within the western boundary current, thus representing the signal propagation along the western boundary. The lead-lag correlation analysis (figure 3.14 - right panel), show a 20-year lag between $40°N$ and $20°N$ which corresponds with the recirculation timescale of the subtropical gyre. Once the signal enters the western boundary waveguide the subsequent equatorward progression is relatively fast. It takes about 45 years for the signal to travel from the northern North Atlantic at $40°N$ and reach the subtropical South Atlantic. This indicates a much faster signal propagation at lower latitudes.

We note, however, that the method used in calculating the lead-lag correlation has certain implications. This is mainly due to the fact that the signal changes quite considerably as it propagates equatorwards. Hence, we infer a time-lag by correlating samples that, though they exhibit a similar structure, are quite different in terms of magnitude and variability. This test might not provide an exact timing of the signal propagation, however it gives a reasonably good estimate of the time-lag between high and low latitudes. Furthermore, the time-lag inferred from this analysis should also be viewed relatively to 3.12, as an approximate indication of the dominant timescales associated with the signal propagation.

The results presented here, show the existence and great importance of the deep western boundary current as an oceanic bridge linking the Northern and Southern Hemisphere. An important part of the result is the steady weakening of the propagating signal associated with the subsurface warming in the Atlantic Ocean. Initially, there is a warming at mid-depth of about 2°C in the North Atlantic, but by the time it has reached the South Atlantic the signal is almost gone. However, this leaves us with the question of how to get the signal to Antarctica, which we will address in the following discussion.

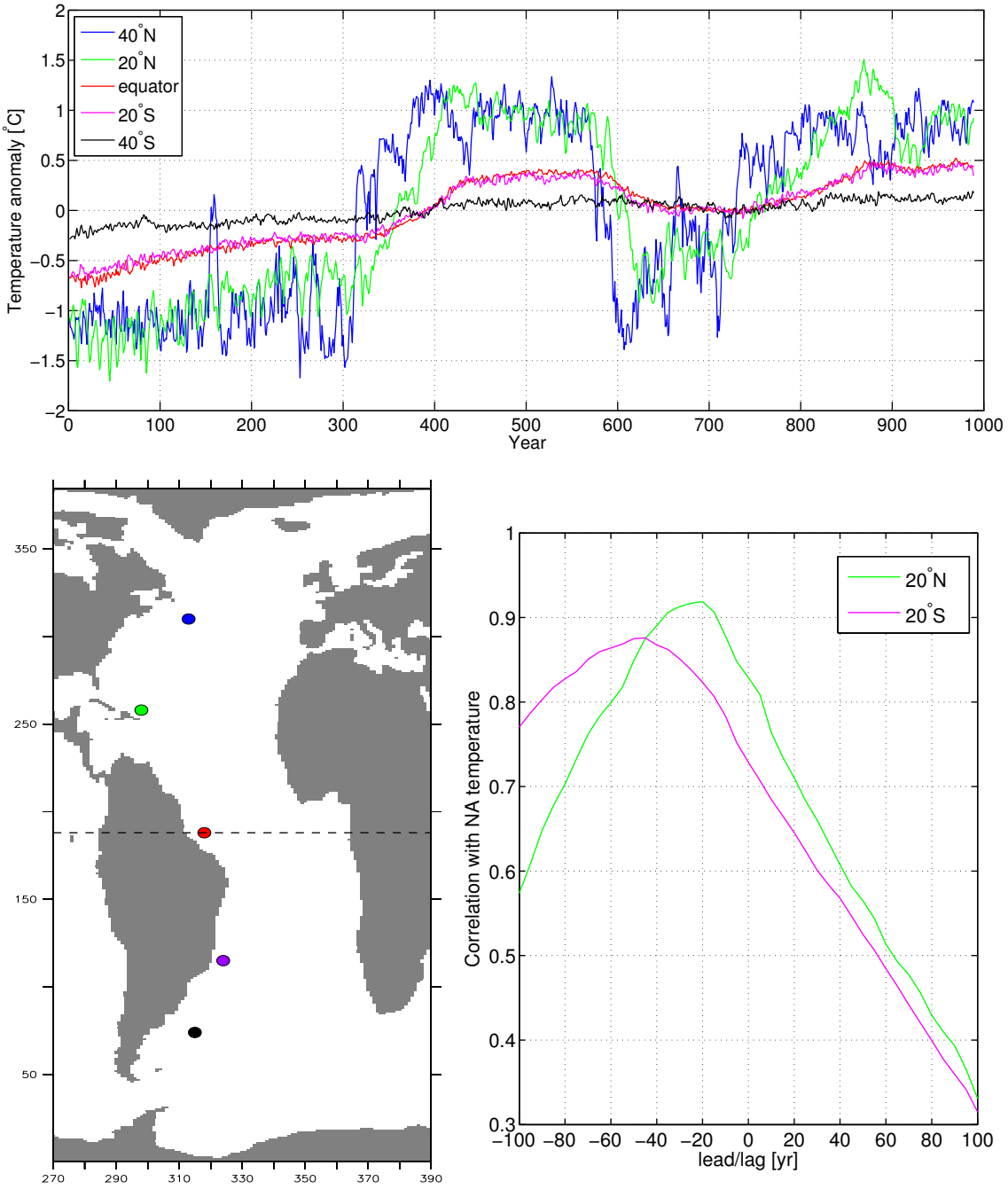

Figure 3.14: *Left* Potential temperature anomalies at 1000 m depth along the western boundary in the Atlantic Ocean, where the colors correspond to different latitudes. *Right* Lead-lag correlation between the different curves in the left figure and the North Atlantic temperature at 40°N corresponding to the inter-gyre boundary (*blue line*). Lead-lag correlation analysis is performed using the North Atlantic signal (blue line in left figure) as a reference, thus assuming that the sub-surface warming is initiated at the western boundary in the northern midlatitudes. We use a lead-lag matrix with values from -100 to 100 in 5 year increments, which basically shift the time series and based on this ensemble of different leads and lags we calculate the maximum correlation with the North Atlantic signal.

Chapter 4

Discussion

In this section we discuss the main results presented in the preceding sections. We focus the first part of the discussion on the possibility of a bipolar see-saw triggered by stochastic climate variability in the tropics. With reference to the previously proposed teleconnection mechanism, we discuss how deep convection in the Southern Ocean can trigger centennial scale climate variability in the Southern Hemisphere. The second part will focus in the results presented in section 3.4 and discuss the role of the Atlantic ocean circulation in mediating a climate signal between the Northern and Southern Hemisphere.

4.0.6 Southern Ocean deep convection as possible trigger for centennial climate variability

The deep convection events in the Weddell Sea is an inherent feature in the CCSM4 pre-industrial simulation, and is remarkably similar to the Weddell Polynya observed in the 1970s. This, apparently rare event, represents a mode of Southern Ocean ventilation that has not been observed since it first was discovered but is still one of the most well-documented climate events in the Southern Ocean. Hence, the Weddell Polynya provides important information about the mechanism associated with deep convection in the Southern Ocean and how it is linked to hemispheric climate variability. One of the biggest differences between the deep convection in CCSM4 and the observed polynya is the spatial extent and location of the convective region. We find that the deep convection occur in the southwestern limb of the Weddell Gyre, whereas the observations of the

Weddell Polynya suggest that the convective region is located far more towards the central median axis (see figure A.4). [Gordon et al., 2007] suggested that the initialization of the Weddell Polynya was linked to topographical effects by Maud Rise.[1] This effect might not be properly resolved by the CCSM4 model and could explain the observed difference. However, our results suggest that the open-ocean deep convection and polynya formation is rather a consequence of changes in the stratification of the Weddell Sea driven by internal climate variability linked to the previously proposed teleconnection mechanism. This is supported by results from an ensemble of CMIP5 models presented in [de Lavergne et al., 2014]. The study shows that 25 out of the 36 models exhibit deep convection and polynya activity in the Southern Ocean under pre-industrial conditions similar to the CCSM4 simulation. The convection is primarily confined to the Weddell Sea, but small regions of convection is also present in the Ross Sea. However, the majority of the CMIP5 models does not capture the details of the observed polynya, which is also true for the CCSM4 simulation. Compared to observations, the sea ice anomaly is not a perfect polynya in the sense that it is not an enclosed region of open ocean within the perennial sea ice pack. Rather, it appears to be more of a general cessation of sea ice in the convective region. The discrepancy between models and observations is most likely linked to the poor representation of the vertical diffusion of salt during sea ice formation, and represent one of the greatest challenges in todays climate models.

It has previously been suggested that deep convection in the Southern Ocean and the formation of polynyas such as the Weddell Polynya can be linked to large scale climate variability in the Southern Hemisphere. [Cheon et al., 2013, Gordon et al., 2007, McKee et al., 2011] One of the principal modes of Southern Hemisphere climate variability is the Southern Annular Mode (SAM), which is dominating the middle to higher latitudes of the Southern Hemisphere on interannual to decadal time scales. The SAM is manifested as meridional shifts of the Southern Hemisphere westerlies that leads to changes in the moisture transport from the midlatitudes to the Southern Ocean. In the negative phase of SAM the westerlies shift towards the equator, which allows for northward expansion of cold, dry polar air masses. This tends to cool the Weddell Sea and reduces the precipitation in the convective region. The cold and dry conditions increase the surface salinity, and the surface water in the Weddell Sea can become sufficiently dense

[1] Maud Rise is a seamount with a 1700-m peak located in the eastern part of the Weddell gyre at $63°–67°S, 2°W–6°E$. Here, local processes affect the upper ocean stratification and induce upwelling in the vicinity of the topographic feature.

to destabilize the pychnocline thus triggering overturning of the water column. This enables deep convection within the Weddell Sea, bringing relatively warm water from the deep ocean to the surface, while cold surface water sinks to the bottom. During the positive phase of SAM the maximum westerlies contracts towards Antarctica resulting in an increased moisture transport into the Weddell Sea region. Hence, deep convection is inhibited by freshening of the surface layer and a weak stratification in the Weddell Sea prevails. Furthermore, surface temperatures over the Weddell Sea tends to increase in response to the increased advection of maritime air masses from lower latitudes. Hence, this sequence reflects how atmospheric changes triggered outside the polar regions can affect the stratification in the Southern Ocean and lead to deep convection as illustrated in figure B.2 taken from [Gordon, 2014].

Our results suggest, however, that the atmospheric circulation changes in the Atlantic sector of the Southern Ocean are directly associated with changes originating in the tropical Pacific region. So, rather than being a connection between middle and high latitudes as hypothesized by the SAM, this mechanism constitutes a direct coupling between the tropics and southern high latitudes. Thus, the tropical-polar teleconnection provides a trigger for changing the surface conditions in the convective region which can lead to destabilization of the water column and convective overturning in the Weddell Sea. This furthermore suggest that deep convection in the model is a result of the stochastic precipitation anomalies in the WTP, which also explains the intermittent nature of the deep convection in the model. This is also consistent with previous studies that highlight the tropical Pacific as a critical region for producing the observed high latitude response and has been shown to account for the recent warming in the continental West Antarctica[Ding et al., 2011].

In section 3.3.2 we show that the open-ocean deep convection in the model is gradually weakening throughout the integration, which appears to be unrelated to a trend in SAM or ENSO-variability. However, [de Lavergne et al., 2014] show that the CMIP5 models show a cessation of open-ocean deep convection as a result to anthropogenic forcing. Under pre-industrial conditions, deep convection in the Southern Ocean is quite common, but gradually weakens due to a warming trend and surface freshening of the Southern Ocean since the beginning of the 20th century. This acts to strengthen the stratification and explains why open-ocean deep convection has not been observed since the Weddell Polynya in the mid-1970's. We speculate, that the decreased trend in Southern Ocean deep convection in the CCSM4 simulation could be linked to similar processes. Hence,

by decreasing the surface salinity by changing the surface freshwater balance (P-E) or a reduction in sea ice production. Changes in the wind-stress could also affect stratification in the convective region by modulating the available potential energy for mixing. However, it remains unexplained, what exactly causes this observed cessation of deep convection in the CCSM4 simulation.

The absence of deep open-ocean convection is a limiting factor of the ventilation of Southern Ocean, which has important implications for Antarctic bottom water formation and could explain the decline in the volume of AABW observed in recent years. [de Lavergne et al., 2014, Robertson et al., 2002] This highlights the role of the Southern Ocean in modifying the global climate through changes in the strength of the overturning circulation and deep ocean heat storage. Model results presented in [Martin et al., 2015], show that formation and northward extent of the AABW depends strongly on the state of the Weddell Sea deep convection which drives a bipolar see-saw between the Southern Ocean and the North Atlantic on multi-centennial timescales. This interhemispheric connection is driven by changes in the AMOC through a competition between northward AABW transport and southward transport of NADW, similar to the idea from [Broecker, 1998], but with the trigger located in the Southern Ocean rather than in the North Atlantic. The see-saw pattern is triggered by changes open-ocean deep convection in the Weddell Sea which is internally driven through stochastic forcing by the atmosphere. In this sense, their simulation is quite similar to the CCSM4 simulation presented here, however their results differ significantly from the ones observed in CCSM4. [Martin et al., 2015] shows that the deep convection exhibits strong multi-centennial climate variability switching between periods with an active deep convection and periods with no convection at all. Hence, the state of the Southern Ocean deep convection appears to be bistable, where the convective and non-convective regimes represents different climate states. During periods of active deep convection, the deep ocean loses a significant amount of heat to the atmosphere, which prohibit the formation of sea ice in the convective region and leads to the formation of an open-ocean polynya. The convective region associated with the polynya is about 4 times bigger compared to the Weddell Polynya observed in the mid-1970's, and consequently the deep ocean is loosing heat on the order of 10^{23}J over a couple of decades.[2] Due to this massive heat flux from the deep ocean, the convective overturning can persist for several decades. Eventually,

[2]In comparison the estimated heat flux associated with the Weddell Polynya is 0.4×10^{21} J/yr.

the heat reservoir is depleted leading to an abrupt shutdown of the deep convection and explains the centennial timescale of the Southern Ocean climate variability. This is quite different from our results in the CCSM4 simulation, which shows that the open-ocean deep convection in the Weddell Sea is significantly weaker and highly intermittent. We show, that the impact of deep convection is primarily confined to the upper 1,000 m of the ocean, with only small changes in temperature in the deep and bottom waters. The results from [Martin et al., 2015], however, is a strong indication that the deep ocean heat reservoir is a necessary condition for maintaining a persistent state of deep convection that can last for several decades. Hence, this points to the fact that we need relatively big and long-lived convective events in order to effectively change the deep ocean heat content and thereby modify the formation of AABW. This further suggests that the state of the Southern Ocean ventilation is highly dependent on the background climate state.

We find, that consecutive deep convection events can be separated by multiple decades, which suggests that some kind of pre-conditioning is needed to trigger deep convection. Here, the stratification of the Weddell Sea is likely to be a controlling factor in setting the time scale. The parameterization of deep convection in the model might also control how sensitive the model is to changes in the surface forcing. The experiments with the CMIP5 models from [de Lavergne et al., 2014], indicate that CCSM4 is a relatively weak convective model compared to other climate models. This could be related to the representation of sea ice formation in the model, which influences the stratification in the Weddell Sea convective region. Our results seem to suggest that the strength of the deep convection is limited by a restoring force triggered by the stochastic atmospheric variability acting to increase stratification. We imagine, if sea ice formation was less sensitive to atmospheric changes, it would be more difficult to restore the stratification and deep convection would not be shutdown so easily.

The exciting results from [Martin et al., 2015] show that deep convection in the Weddell Sea can trigger centennial climate variability, but without explicitly accounting for the initial trigger of the deep convective events. However, a number of recent studies, including the present one, show a teleconnection between tropical climate variability and changes in the atmospheric circulation over the Weddell Sea, thus providing the initial trigger for destabilizing the water column in the convective region. We note, however, that the comparison with [Martin et al., 2015] and [de Lavergne et al., 2014] indicate

that the Southern Ocean deep convection in CCSM4 is too weak to cause long-term trends in the Southern Hemisphere climate. We argue, that this could be related to the stratification in the Weddell Sea and is strongly dependent on the climatic background state. Furthermore, the size of the deep ocean heat reservoir is an essential key in sustaining the weak stratification and ensure deep convection on decadal to centennial timescales. We note, however, that the ocean-air heat flux, necessary for maintaining deep convection on centennial timescales, is significantly bigger than suggested by any observations and might represent an unrealistically large amount of heat stored in the deep ocean. Furthermore, the deep ocean heat storage is thought to have changed considerably during the last glacial, which could also impact the strength of the Southern Ocean deep convection.

4.1 Ocean circulation changes in the Atlantic

4.1.1 Chiang hypothesis

[Chiang et al., 2008, Chiang and Bitz, 2005] proposed an atmosphere-surface ocean teleconnection that explains the asymmetric hemispheric response associated with cooling in the North Atlantic. Their proposed teleconnection mechanism is characterized by an initial ocean adjustment in the North Atlantic midlatitudes as a result of AMOC slowdown followed by a fast atmospheric response driving a southward shift in the tropical Atlantic ITCZ and subsequent warming in the South Atlantic.

A similar mechanism is described in [Lee et al., 2011], who show intensification of Southern Hemisphere midlatitude westerlies in response to surface cooling in the North Atlantic and subsequent southward displacement of the Atlantic ITCZ. This influences the strength of the Southern Hemisphere westerlies through changes in the Hadley circulation. The strengthening of the westerlies causes an increased northward Ekman transport in the surface layer which is compensated by upwelling from depths[Toggweiler and Samuels, 1995]. This causes stronger deep ocean ventilation and outgassing of CO_2 thus providing an explanation for the glacialinterglacial CO_2 variation [Anderson et al., 2009]. Hence, this atmospheric teleconnection mechanism, manifested as a shift in the tropical Atlantic ITCZ, describes a pathway that transmits the North Atlantic climate signal to the Southern Ocean.

In section 3.4.3 we described a similar pattern in the tropical Atlantic response to cooling in the North Atlantic occurring in a preindustrial simulation of CCSM4. Similar to [Chiang et al., 2008], the initial adjustment is dominated by a surface ocean cooling in the northern high latitudes due to an ocean-atmosphere feedback mechanism associated with a slowdown of the AMOC. The Southern Hemisphere response is characterized by a weak surface warming in the midlatitudes and a southward shift in the tropical precipitation. We note, however, that the atmospheric changes observed in the CCSM4 simulation are relatively small in magnitude compared to [Chiang et al., 2008, Lee et al., 2011], who both use a prescribed forcing to trigger North Atlantic cooling. [Lee et al., 2011] use a prescribed cooling of the North Atlantic corresponding to a flux of 120 W/m2 applied everywhere north of 25°N in the Atlantic, which is noted to be somewhat high. This causes a strong and widespread cooling throughout the Northern Hemisphere, averaging around 4°C, and surface air temperatures in the North Atlantic decrease by up to 12°C. Consequently the changes in tropical Atlantic precipitation is about a factor of 10 larger (i.e. $1.5 - 2.0$ cm/day) compared to the response in the CCSM4 simulation. The same is evident in [Chiang et al., 2008], which shows extensive surface cooling in the Northern Hemisphere triggered by an abrupt freshening of the North Atlantic.

Hence, we argue that the strong response in these models is due to the relatively large prescribed forcing. A common feature of most climate models is that they require an unrealistically large forcing in order to produce a temperature response, that is in agreement with paleo-proxies [Lang et al., 1999]. Hence, they might overestimate the sensitivity and relative strength of the different feedback mechanism associated with the forcing. However, in an unforced model, the initial "kick" is caused by internal climate variability and the response is therefore also expected to be significantly smaller since the magnitude of the response depends largely on a strong feedback mechanism to amplify the initial perturbation.

This, altogether, suggest that we need quite a large perturbation and strong positive feedback mechanisms to effectively change the atmospheric circulation in the tropical Atlantic and trigger increased wind-driven upwelling and deep ventilation of the Southern Ocean.

4.1.2 Signal propagation in the Atlantic Ocean

The recent observations from WAIS suggest an anti-phase relation between Greenland and Antarctica with a northern lead of about 200 years, which strongly suggests a connection through the ocean. Prior to these recent findings, it was suggested that a characteristic timescale could be set by heat equilibration in the Southern Ocean [Stocker and Johnsen, 2003]. However, this suggested a timescale of about 1,000–1,500 years corresponding to an Antarctic lead as found in [Blunier and Brook, 2001] which is inconsistent with the recent results from WAIS. The classic bipolar see-saw [Broecker, 1998, Crowley, 1992] implied that changes in the north and south occur at the same time, which requires a very fast signal transmission in the ocean. This is possible through fast wave adjustment processes with a characteristic timescale of months to a couple of decades. Here, the lag in Antarctic temperatures, inferred from the recent synchronization of Greenland and Antarctic ice cores, is attributed to the slow propagation in the Southern Ocean. This view is generally accepted as the leading hypothesis of the bipolar see-saw and the basis for a great number of modeling studies. However, the majority of the current modelling studies does not readily account for the processes, through which the temperature signal is transmitted to high southern latitudes, let alone how to get the signal across the Southern Ocean to Antarctica.

In the previous section we showed that the subsurface warming signal in the Atlantic was associated with a reduction in the gyre circulation with subsequent heat convergence in the upper cell of the AMOC. At the surface this corresponded to a widespread cooling in the North Atlantic north of 40°N with a $10 - 12$°C decrease in temperature locally. We noted, that this pattern of strong surface cooling in the North Atlantic and the associated subsurface warming spreading into the South Atlantic, is somewhat similar in nature to the aforementioned bipolar see-saw response. The propagation north of 20°N is determined by the gyre circulation, which suggests a time scale of about 20 years.[3] It takes about 45 years for the warming signal to reach the subtropical South Atlantic, which is illustrated in figure 3.12 and by the lead-lag correlation analysis.
[Kawase, 1987] shows that the fast ocean adjustment is determined by a Kelvin wave propagating anticlockwise along the boundaries and subsequently radiating Rossby waves

[3] A rough estimate of the re-circulation in the subtropical gyre yields a typical timescale of about 20 years. Taking the width of the North Atlantic to be $L = 3000km$ and a typical horizontal speed of $U = 1cm/s$, we get: $t = 2L/U = 6 * 10^6/(1 * 10^{-2} * 60 * 60 * 24 * 365) \approx 20years$.

into the interior from the eastern boundary. The fast baroclinic ocean adjustment would lead to an almost in-phase relationship between high and low latitudes. In general the Kelvin wave response is relatively fast, with a typical propagation time on the order of a couple of months [Johnson and Marshall, 2002]. The Rossby wave response is significantly slower and is highly dependent on the vertical structure of the ocean. Hence, the baroclinic response can be on the order of a couple of months, whereas the barotropic response is significantly slower, i.e. up to several years. However, the time lag of 45 years between 40°N and 20°S, suggest that advective processes rather than the much faster wave adjustment controls the signal propagation. The signal propagation illustrated in figure 3.12 shows the steady advection across the equator guided by the deep western boundary current. However, from wave theory it is evident, that the Kelvin wave cannot cross the equator on the western boundary, since the pressure gradient can no longer be balanced. This further indicates that the signal propagation is an advective process, resulting in a time lead of several decades between the subpolar and subtropical Atlantic.

[Getzlaff et al., 2005, Johnson and Marshall, 2002] show that the meridional signal propagation, associated with changes in the Atlantic overturning circulation, is largely dependent on the model resolution. Experiments with a high-resolution (1/3°) eddy-permitting model show a significantly higher propagation speed compared to the low resolution model with a (4/3°) horizontal resolution. Thus, in the eddy-permitting version the propagation from high to low latitudes is on the order of a few months, which is indicative of a fast Kelvin wave response along the western boundary. The non-eddy resolving model shows a much slower propagation speed of several years related to slow advective processes. In the subtropics, however, the propagation speed is significantly higher, which matches with our results that show a fast propagation between the equator and 20°S compared to the slow response in the Northern and Southern Hemisphere mid-latitudes. However, we note that the 1° resolution in the ocean component of CCSM4, might be too coarse to properly resolve the fast Kelvin wave response and could explain why advection is the dominating response. The results from [Getzlaff et al., 2005, Johnson and Marshall, 2002] thus indicate that model resolution is a key aspect in setting the timescales for signal propagation in the ocean. Hence, increasing the horizontal resolution could provide a fast ocean interconnection mechanism through wave adjustment processes, that would lead to an almost in-phase relationship between northern and southern high latitudes.

In light of the observations from WAIS, we should expect a lag of about 200 years between Greenland and Antarctic temperatures. Hence, the relatively fast signal propagation from the high to low latitudes, would suggest that the Southern Ocean is important in setting the timescale of the bipolar see-saw response. It is generally believed that the ACC acts as a barrier against meridional flow thus limiting the poleward ocean heat transport onto Antarctica. Hence, Antarctica appears to be both thermally and dynamically isolated from lower latitudes, and the question remains how to get the subsurface warming signal across the ACC. A study by [Schmittner et al., 2003], shows that the meridional propagation of a temperature signal is mainly determined by the strength of the ACC. In the standard experiment, the Southern Ocean circulation is dominated by the surface wind-stress. Here, it takes about 400-500 years for a warming signal in the North Atlantic to reach high latitudes in the Southern Hemisphere. This time scale is primarily set by the presence of the ACC, hindering further southward flow. The key reason behind the slow propagation across the ACC is the absence of lateral boundaries, which prohibits propagation of fast boundary waves thus isolating Antarctica from the regions north of the ACC.

The results from our comparison with [Stommel and Arons, 1959–1960] as well as [Kawase, 1987] show that the western boundary is essential in communicating a signal from the North Atlantic to the Southern Hemisphere. As described earlier the subsurface warming signal is gradually weakening as it propagates southward in the deep western boundary current. By the time it reaches the South Atlantic midlatitudes the magnitude of the signal is significantly reduced and further southward propagation is inhibited by the presence of the ACC. We note that the warming signal starts out as a 2°C anomaly in the North Atlantic, but is almost non-existing when it reaches the South Atlantic midlatitudes and is completely consumed by the vigorous flow of the ACC. This implies, that we would need a substantially larger perturbation in the North Atlantic in order to get the across the ACC.

Due to the lack of zonal boundaries the propagation across the ACC must be governed by different processes which constrain the lag between Northern and Southern Hemisphere. The strength of the circumpolar transport is largely set by the energy input from the strong westerlies in the Southern Ocean leading to baroclinic instability which is balanced by generation of eddies. Thus variations in the strength of the ACC has typically been linked to changes in the Southern Ocean wind-stress, as in [Schmittner et al., 2003] who show a significantly weakened ACC transport by reducing the Southern

Ocean wind-stress, leading to a faster meridional propagation across the ACC with a suggested timescale of 200 years. However, recent studies might suggest that the ACC transport is remarkably insensitive to changes in the wind-stress forcing due to eddy compensation processes [Hogg et al., 2015, Munday et al., 2012].

Eddies in the Southern Ocean play a key role in modulating the ocean circulation response to surface forcing and are therefore key in understanding the dynamics of the ACC, through their ability of transferring momentum and heat fluxes across the ACC. [Hogg et al., 2015, Marshall and Speer, 2012, Munday et al., 2012]. Experiments with high-resolution models show that the eddy compensation is largely dependent on the horizontal resolution and primarily acts to counterbalance the potential energy put into the surface by the wind. Thus, eddy-transport in the ACC can compensate changes in the northward Ekman transport leading to little changes in the residual transport. The total effect of the eddies, however, is still relatively unknown, but current studies indicate that they are an important feature of the circulation in the Southern Ocean and might provide a mechanism of fast signal propagation across the ACC.

Chapter 5

Summary and conclusion

Temperature reconstructions from ice core records in Greenland show the occurrence of several abrupt climate transitions during the last glacial period. This remarkable feature in the Greenland climate record, known as Dansgaard-Oeschger events, also have counterparts in the Antarctic ice core record, revealing an interhemispheric coupling of the Northern and Southern Hemsiphere during the last glacial.

In this study we present the results from a pre-industrial control simulation of CCSM4, showing a series of unforced and abrupt climate transitions in the North Atlantic, which closely resembles the characteristic signature of a Dansgaard-Oeschger event. This simulation thus presents a unique insight into the processes and feedback mechanisms related to the abrupt climate transitions, without any presumptions about the initial trigger.

The climate transitions in the model are associated with a persistent El Niño-La Niña pattern, expressed through changes in precipitation over the western tropical Pacific, triggering a persistent pattern in sea level pressure above the North Atlantic. We show a similar atmospheric teleconnection between the tropics and southern high latitudes, manifested as an out-of-phase relationship between SLP anomalies in the South Atlantic sector of the Southern Ocean and precipitation in the western tropical Pacific. The initial trigger is the stochastic precipitation anomalies caused by anomalous heating in the tropical Pacific, which is readily communicated via a stationary Rossby wave response to both northern and southern high latitudes. Hence, this teleconnection mechanism constitutes a fast communication of tropical climate variability to the polar regions through the atmosphere.

In the North Atlantic a strong feedback loop, causes a transition in North Atlantic climate which persists on centennial time scales. However, in the Southern Hemisphere the climate response associated with the tropical forcing, is much weaker and does not persist on time scales longer than a few decades. This is explained by the absence of a strong feedback mechanism in the Southern Hemisphere, which is necessary to amplify the initial trigger in the tropics.

Motivated by a recent study by [Martin et al., 2015], we explore the potential for deep convection in the Southern Ocean as a trigger for centennial climate variability in the Southern Hemisphere. We find that open-ocean deep convection in the Weddell Sea is a persistent feature in the pre-industrial control simulation of CCSM4 and exhibit a similar structure as the Weddell Polynya observed in the mid-1970's. However, the convective events are too weak and short-lived to cause significant warming of the deep water in the Weddell Sea, which is a necessary condition for changing the AABW formation and effectively ventilating the deep ocean [Robertson et al., 2002]. We suggest, that the relatively weak state of Southern Ocean deep ventilation is due to a strong influence of sea ice on the Weddell Sea stratification, which prevents the evolution of strong deep convection. We thus conclude, that by affecting the atmospheric circulation at high southern latitudes, precipitation anomalies in the central and western tropical Pacific may account for the observed variability in open-ocean deep convection in the Weddell Sea.

Our analysis suggests, that the strong and persistent state of deep convection in the Southern Ocean observed in [Martin et al., 2015] is linked to the massive ocean-atmosphere heat flux associated with the anomalously large convective area and represents an upper limit for the state of deep convection in the Southern Ocean. We note that the magnitude of the heat flux might be slightly unrealistic, which explains why the deep convection observed in CCSM4 does not exhibit any long term climate variability. However, combining the current knowledge on Southern Ocean deep convection from [de Lavergne et al., 2014, Gordon et al., 2007, Martin et al., 2015] and the influence of tropical climate variability on southern high latitude climate [Ding et al., 2011, McKee et al., 2011, Robertson et al., 2002, Trenberth et al., 1998] we show a potential mechanism for the tropical-polar teleconnection as a trigger for open-ocean deep convection in the Southern Ocean. Hence, this propose a "new" mechanism for the north-south coupling that links deep convection and Southern Ocean ventilation to changes in the general overturning circulation through stochastic tropical climate variability.

Next, the we examined the ocean circulation adjustment in the Atlantic following an abrupt climate transition and cooling in the North Atlantic described in [Kleppin et al., 2015]. Initial weakening of the subpolar gyre, driven by an ocean-atmosphere feedback mechanism, results in slowdown of the AMOC by 3-4 Sv with consequent heat convergence at the subtropical-subpolar gyre boundary. This leads to a strong surface cooling in the northern North Atlantic, while a warming anomaly evolves in the subsurface of the midlatitudes. Subsequent equatorward progression is dominated by a slow ocean adjustment, leading to an asymmetric response in the subsurface temperatures between North Atlantic and the South Atlantic midlatitudes. This was in contrast to [Chiang et al., 2008, Lee et al., 2011], where the response was dominated by an atmosphere-surface ocean mechanism resulting in an southward displacement of the tropical Atlantic ITCZ and increased wind-driven upwelling in the Southern Ocean. However, the results presented here, suggested that the relatively weak cooling of the Northern Hemisphere, resulting from the weak AMOC response, was insufficient to cause significant changes to the tropical ITCZ. We argue that the strong atmospheric response found in [Chiang et al., 2008, Lee et al., 2011], might be a result of the relatively large forcing which is prescribed in these models and highlights the consequences of external forcing versus internal climate variability.

We show that the propagation of the warming signal in the North Atlantic mid- and high latitudes is dominated by a slow advective flow in the subtropical gyre, with a characteristic time scale of about 20 years. The southward propagation of the warm anomaly is confined to the western boundary, where the signal propagation is considerably faster, and the warming anomaly reaches 20°S after about $\approx$ 45 years. This time scale is consistent with the slow tracer advection time scale, rather than the fast Kelvin wave response and is consistent with [Stommel and Arons, 1959–1960], who predicted this cross equatorial flow in the deep western boundary current. The warming anomaly is gradually weakening by advective-diffusive processes as the signal propagates through the Atlantic. When the signal reaches 40°S, the anomaly has decreased by almost 70% relatively to the North Atlantic. Further southward propagation is inhibited by the ACC, acting as a barrier against meridional flow. Hence, the temperature signal does not make it across to Antarctica, which we argue is due to a combination of the strong weakening of the warm anomaly as the signal spreads through the Atlantic and the presence of the ACC. The strong attenuation of the temperature signal, is an indication that we need a substantially larger initial pertubation in the North Atlantic if we hope to get

an advective signal across the ACC. This further suggests that the dynamics associated with the ACC transport are an essential factor in setting the time scale for the north-south coupling and put the Southern Ocean into the centre stage of interhemispheric climate variability in the past and in the future.

Appendix A

Additional figures

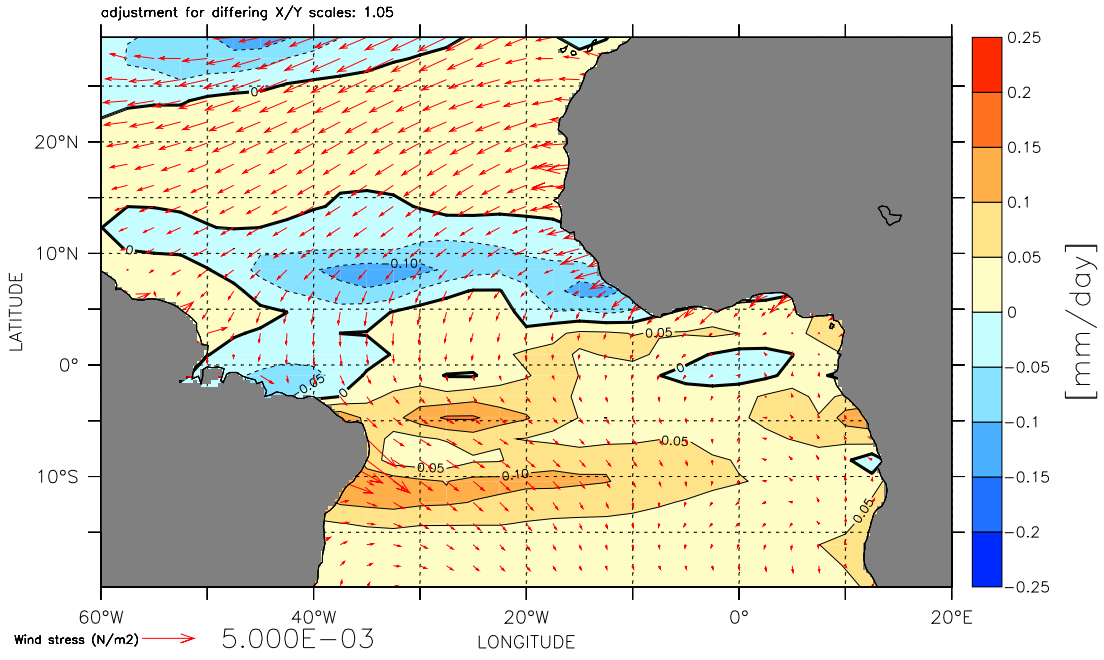

Figure A.1: Difference in precipitation (shading; mm/day) and wind-stress (vectors; N/m2) between the cold (year 400-550) and the warm phase (year 50-250) over the tropical Atlantic region. Vectors correspond to the zonal and meridional components of the anomalous wind-stress and a reference vector of length ($0.005 N/m2$) is plotted in the lower left corner for comparison. Contour interval is 0.05 mm/day. The precipitation anomalies are indicative of a southward shift of the marine ITCZs.

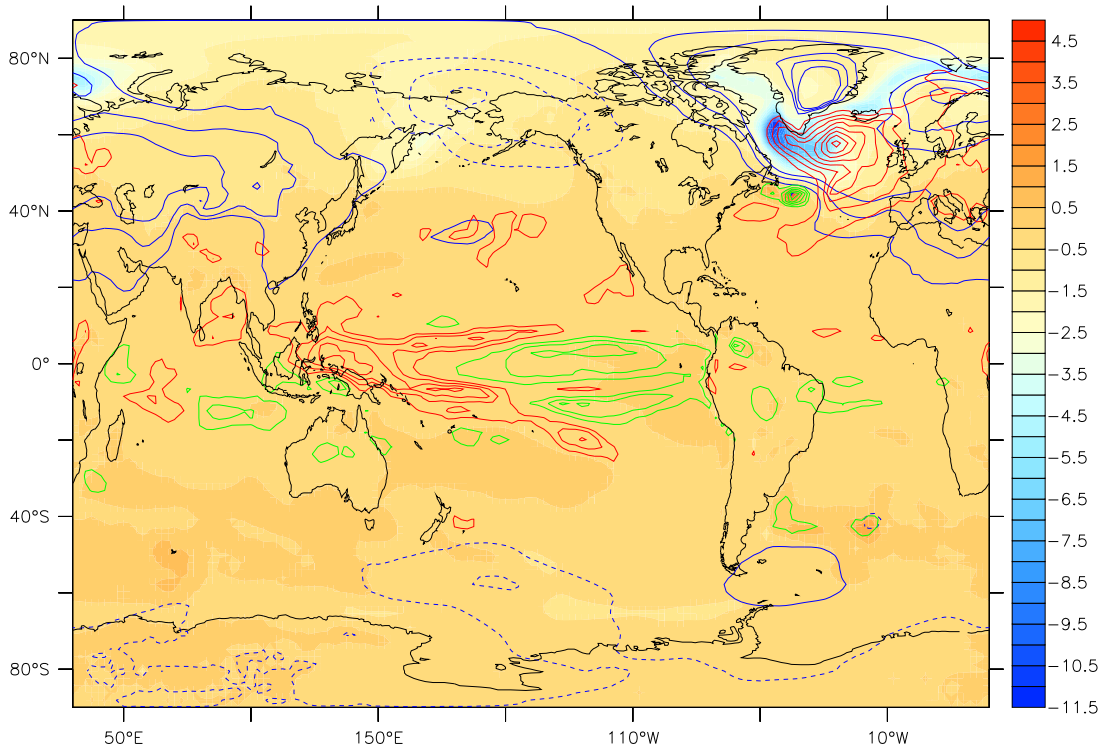

Figure A.2: Surface temperature, sea level pressure and precipitation anomalies for North Atlantic cooling event. Surface temperature (shading; °C), sea level pressure (blue contours in hPa; negative values are dashed) and precipitation (green contours ≥ 0.1mm/day; red contours ≤ -0.1mm/day). Anomalies are averaged over years 400-550 (NA cold state) and years 50-250 (NA warm state)

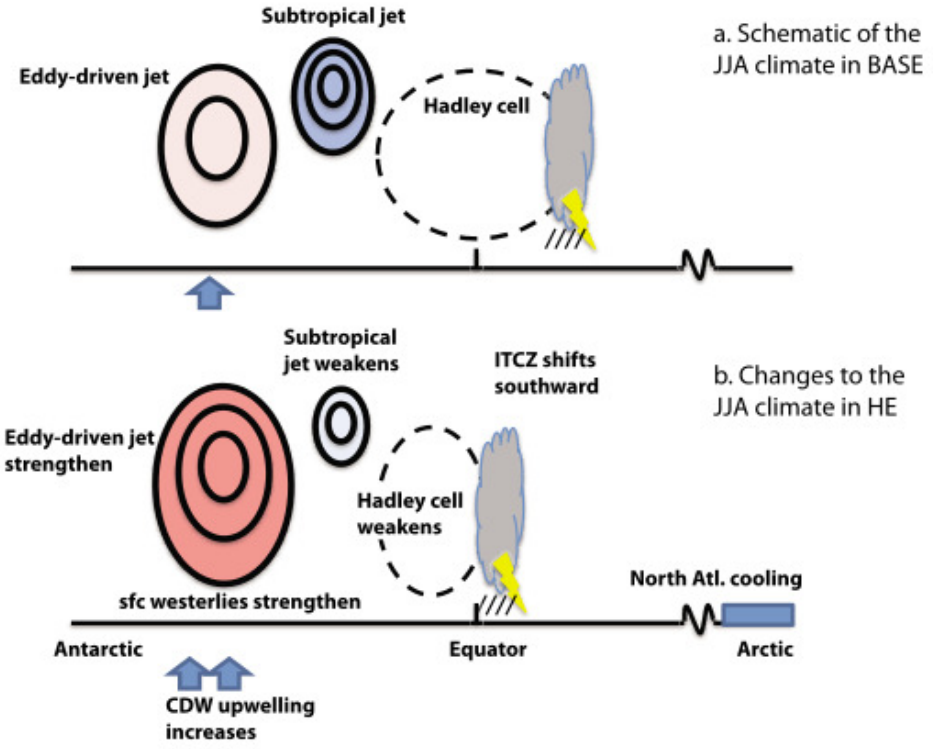

Figure 10. Schematics of the JJA climate in BASE experiment and changes to the JJA climate in HE that illustrate the proposed north-south teleconnection. When the North Atlantic is forced to cool, the CCM3-RGO responded with a southward-shifted ITCZ and increased Southern Ocean midlatitude surface (sfc) westerlies. Other studies have shown that an increase in wind stress leads to a stronger ACC which consequently brings CDW from greater depths.

Figure A.3: Illustration adopted from [Lee et al., 2011] showing the teleconnection mechanism between the North Atlantic and the Southern Ocean. This two-step mechanism can be summerized as follows; (1) in response to the North Atlantic cooling, the tropical ITCZ shifts southward, weakening the southern branch of the Hadley circulation. (2) the weakened southern Hadley cell causes a reduction in the strength of the Southern Hemisphere subtropical jet and in response the Southern Hemisphere midlatitude westerlies increase.

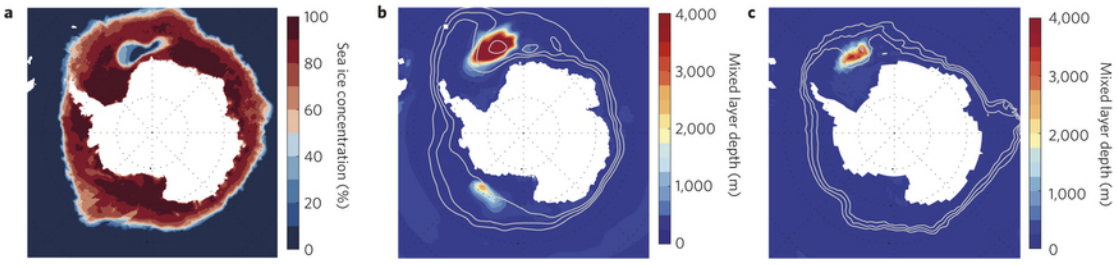

Figure A.4: **a**, Observed 1974–1976 mean September sea ice concentration (%) from Nimbus-5 ESMR Polar Gridded Sea Ice Concentrations delineating the Weddell Polynya extent. **b**, September mixed layer depth (shading) and 25%, 50% and 75% September sea ice concentration contours (grey lines) in the MPI-ESM-LR model, averaged over pre-industrial control years during which the convection area exceeds half of its overall maximum. **c**, The same as in **b**, but for the HadGEM2-ES model. Deep mixed layers, coinciding with anomalously low sea ice concentrations, are found over an area of comparable size to the Weddell Polynya and in a similar location.

Appendix B

Southern Annular Mode (SAM)

The Southern Annular Mode is a hemispheric pattern of climate variability and impacts climate throughout the most of the Southern Hemisphere. Analogous to SAM is the Northern Annular Mode in the Northern Hemisphere. The NAM is associated with large anomalies in Arctic sea ice distribution and sea surface temperatures in the North Atlantic. Hence, the annular modes is one of the most important features of large scale climate variability in the extratropics. The SAM index is usually defined as the difference in the zonal mean sea level pressure between 40°S and 60°S, and describe the anomalous atmospheric flow, that is not associated with the seasonal cycle, between the polar regions and middle latitudes. In the wind field, the SAM is characterized by meridional shifts of the circumpolar westerlies and accounts for 20-30% ann of the total variance in Southern Hemisphere climate variability. Hence, variations in the SAM have a great impact on Antarctic climate through changes in the atmospheric flow. This links SAM to variations in temperatures over Antarctica, changes in sea ice distribution and sea surface temperatures in the Southern Ocean.

In the CCSM4 run there are no significant correlation between the deep convection events and changes to the trend in SAM. Here, we define SAM as the annually averaged difference in zonal mean SLP between 40°S and 65°S. The signal to noise ration is very high with a great deal of interannual variability with a SAM-index ranging from +4 to -8.

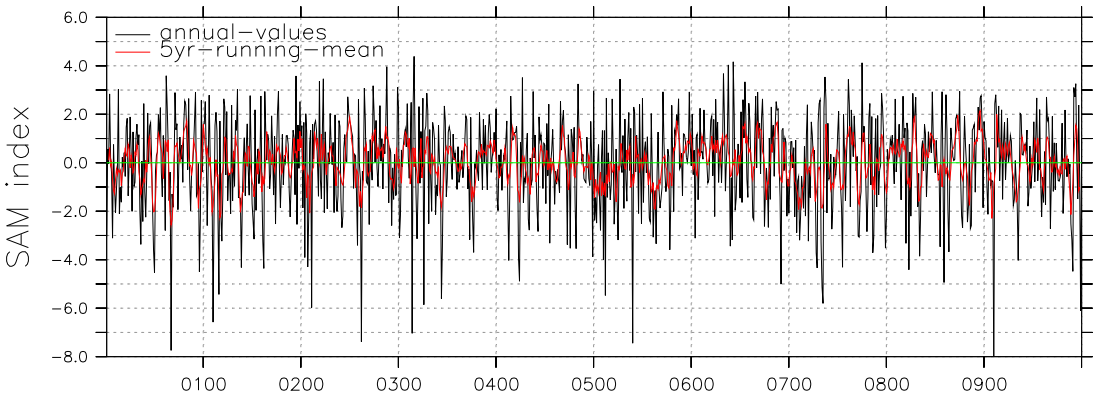

Figure B.1: SAM time series based on zonally averaged SLP indices between 40°S and 65°S. Yearly values are shown as the black line connecting annual values. The red line denotes the 5-yr running mean.

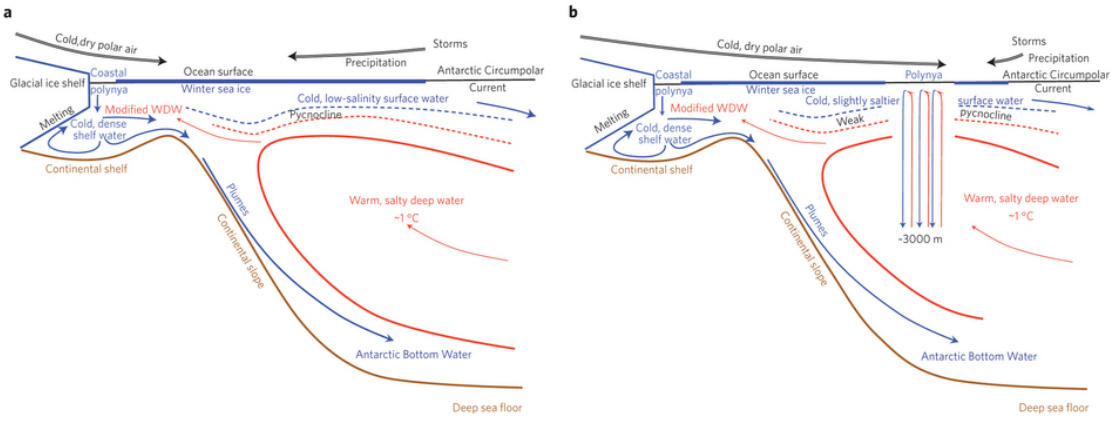

Figure B.2: Schematic from [Gordon, 2014] showing convection in the Southern Ocean during positive and negative phases of SAM. **Left**) The prevailing conditions of the present-day Southern Ocean is one of low-density surface water resting over warmer, saltier, denser deep water within the winter sea-ice cover. Deep-reaching convection is inhibited by precipitation associated with storms of the circumpolar belt. The predominant form of ventilation is limited to the descent of dense water plumes drawn from shelf water masses formed over the continental slope, through a combination of sea-ice generation within a coastal polynya and ocean–glacial ice interaction. **Right**) Northward expansion of cold, dry polar air masses of Antarctica, occurring during a negative Southern Annular Mode, reduces precipitation, increasing surface water salinity, causing a break down of the pycnocline, enabling deep-reaching convection cells that transfer deep ocean heat into the surface layer, while cold surface water reaches into the deep ocean, resulting in a winter polynya, and an alternative mode of deep ocean ventilation. WDW - warm deep water.

Bibliography

Annular modes website. http://www.atmos.colostate.edu/ao/introduction.html. Accessed: 2015-04-27.

Tropical-extratropical teleconnections: Pna and psa. https://www.ipcc.ch/publications_and_data/ar4/wg1/en/ch3s3-6-2-2.html. Accessed: 2015-03-30.

Global precipitation and enso. http://precip.gsfc.nasa.gov/rain_pages/el_nino_vsn2.html. Accessed: 2015-03-27.

R. F. Anderson, S. Ali, L. I. Bradtmiller, S. H. H. Nielsen, M. Q. Fleisher, B. E. Anderson, and L. H. Burckle. Wind-driven upwelling in the southern ocean and the deglacial rise in atmospheric co2. *Science*, 323(5920):1443–1448, 2009. doi: 10.1126/science.1167441.

C. Barbante, J.-M. Barnola, S. Becagli, J. Beer, M. Bigler, C. Boutron, T. Blunier, E. Castellano, O. Cattani, J. Chappellaz, D. Dahl-Jensen, M. Debret, B. Delmonte, D. Dick, S. Falourd, S. Faria, U. Federer, H. Fischer, J. Freitag, A. Frenzel, D. Fritzsche, F. Fundel, P. Gabrielli, V. Gaspari, R. Gersonde, W. Graf, D. Grigoriev, I. Hamann, M. Hansson, G. Hoffmann, M. A. Hutterli, P. Huybrechts, E. Isaksson, S. Johnsen, J. Jouzel, M. Kaczmarska, T. Karlin, P. Kaufmann, S. Kipfstuhl, M. Kohno, F. Lambert, Anja Lambrecht, Astrid Lambrecht, A. Landais, G. Lawer, M. Leuenberger, G. Littot, L. Loulergue, D. Lüthi, V. Maggi, F. Marino, V. Masson-Delmotte, H. Meyer, H. Miller, R. Mulvaney, B. Narcisi, J. Oerlemans, H. Oerter, F. Parrenin, J.-R. Petit, G. Raisbeck, D. Raynaud, R. Röthlisberger, U. Ruth, O. Rybak, M. Severi, J. Schmitt, J. Schwander, U. Siegenthaler, M.-L. Siggaard-Andersen, R. Spahni, J. P. Steffensen, B. Stenni, T. F. Stocker, J.-L. Tison, R. Traversi, R. Udisti, F. Valero-Delgado, M. R. van den Broeke, R. S. W. van de Wal, D. Wagenbach, A. Wegner, K. Weiler, F. Wilhelms, J.-G. Winther, and E. Wolff. One-to-one coupling

of glacial climate variability in greenland and antarctica. *Nature*, 444(7116):195–198, 2006. doi: 10.1038/nature05301. URL http://dx.doi.org/10.1038/nature05301.

Joseph J. Barsugli and Prashant D. Sardeshmukh. Global atmospheric sensitivity to tropical sst anomalies throughout the indo-pacific basin. *Journal of Climate*, 15(23):3427–3442, Dec 2002. ISSN 0894-8755. doi: 10.1175/1520-0442(2002)015⟨3427:GASTTS⟩2.0.CO;2. URL http://dx.doi.org/10.1175/1520-0442(2002)015<3427:GASTTS>2.0.CO;2.

Michael Bender, Todd Sowers, Mary-Lynn Dickson, Joseph Orchardo, Pieter Grootes, Paul A. Mayewski, and Debra A. Meese. Climate correlations between greenland and antarctica during the past 100,000 years. *Nature*, 372(6507):663–666, 1994. doi: 10.1038/372663a0. URL http://dx.doi.org/10.1038/372663a0.

T. et al. Blunier. Asynchrony of antarctic and greenland climate change during the last glacial period. *Nature*, 394(6695):739–743, August 1998.

Thomas Blunier and Edward J. Brook. Timing of millennial-scale climate change in antarctica and greenland during the last glacial period. *Science*, 291(5501):109–112, 2001. doi: 10.1126/science.291.5501.109. URL http://www.sciencemag.org/content/291/5501/109.abstract.

Wallace S. Broecker. Paleocean circulation during the last deglaciation: A bipolar seesaw? *Paleoceanography*, 13(2):119–121, 1998. ISSN 1944-9186. doi: 10.1029/97PA03707. URL http://dx.doi.org/10.1029/97PA03707.

Woo Geun Cheon, Young-Gyu Park, J. R. Toggweiler, and Sang-Ki Lee. The relationship of weddell polynya and open-ocean deep convection to the southern hemisphere westerlies. *Journal of Physical Oceanography*, 44(2):694–713, Oct 2013. doi: 10.1175/JPO-D-13-0112.1. URL http://dx.doi.org/10.1175/JPO-D-13-0112.1.

John C. H. Chiang, Wei Cheng, and Cecilia M. Bitz. Fast teleconnections to the tropical atlantic sector from atlantic thermohaline adjustment. *GEOPHYSICAL RESEARCH LETTERS*, 35(L07704), April 2008.

John C.H. Chiang, Shih-Yu Lee, Aaron E. Putnam, and Xianfeng Wang. South pacific split jet, {ITCZ} shifts, and atmospheric north–south linkages during abrupt climate changes of the last glacial period. *Earth and Planetary Science Letters*, 406(0):233 –

246, 2014. ISSN 0012-821X. doi: http://dx.doi.org/10.1016/j.epsl.2014.09.012. URL http://www.sciencedirect.com/science/article/pii/S0012821X14005676.

JohnC.H. Chiang and CeciliaM. Bitz. Influence of high latitude ice cover on the marine intertropical convergence zone. *Climate Dynamics*, 25(5):477–496, 2005. ISSN 0930-7575. doi: 10.1007/s00382-005-0040-5. URL http://dx.doi.org/10.1007/s00382-005-0040-5.

Thomas J. Crowley. North atlantic deep water cools the southern hemisphere. *Paleoceanography*, 7(4):489–497, 1992. ISSN 1944-9186. doi: 10.1029/92PA01058. URL http://dx.doi.org/10.1029/92PA01058.

Gokhan Danabasoglu, Susan C. Bates, Bruce P. Briegleb, Steven R. Jayne, Markus Jochum, William G. Large, Synte Peacock, and Steve G. Yeager. The ccsm4 ocean component. *Journal of Climate*, 25(5):1361–1389, Aug 2011. ISSN 0894-8755. doi: 10.1175/JCLI-D-11-00091.1. URL http://dx.doi.org/10.1175/JCLI-D-11-00091.1.

Casimir de Lavergne, Jaime B. Palter, Eric D. Galbraith, Raffaele Bernardello, and Irina Marinov. Cessation of deep convection in the open southern ocean under anthropogenic climate change. *Nature Clim. Change*, 4, 4 2014. URL http://dx.doi.org/10.1038/nclimate2132.

Gaudenz Deplazes, Andreas Luckge, Larry C. Peterson, Axel Timmermann, Yvonne Hamann, Konrad A. Hughen, Ursula Rohl, Carlo Laj, Mark A. Cane, Daniel M. Sigman, and Gerald H. Haug. Links between tropical rainfall and north atlantic climate during the last glacial period. *Nature Geoscience*, 6(1752-0894), March 2013.

Qinghua Ding, Eric J. Steig, David S. Battisti, and Marcel Kuttel. Winter warming in west antarctica caused by central tropical pacific warming. *Nature Geosci*, 4(6):398–403, Jun 2011. ISSN 1752-0894. doi: 10.1038/ngeo1129. URL http://dx.doi.org/10.1038/ngeo1129.

Trond M. Dokken, Kerim H. Nisancioglu, Camille Li, David S. Battisti, and Catherine Kissel. Dansgaard-oeschger cycles: Interactions between ocean and sea ice intrinsic to the nordic seas. *Paleoceanography*, 28(3):491–502, 2013. ISSN 1944-9186. doi: 10.1002/palo.20042. URL http://dx.doi.org/10.1002/palo.20042.

Peter R. Gent, Gokhan Danabasoglu, Leo J. Donner, Marika M. Holland, Elizabeth C. Hunke, Steve R. Jayne, David M. Lawrence, Richard B. Neale, Philip J.

Rasch, Mariana Vertenstein, Patrick H. Worley, Zong-Liang Yang, and Minghua Zhang. The community climate system model version 4. *Journal of Climate*, 24 (19):4973–4991, Apr 2011. ISSN 0894-8755. doi: 10.1175/2011JCLI4083.1. URL http://dx.doi.org/10.1175/2011JCLI4083.1.

J. Getzlaff, C. W. Böning, C. Eden, and A. Biastoch. Signal propagation related to the north atlantic overturning. *Geophysical Research Letters*, 32(9):n/a–n/a, 2005. ISSN 1944-8007. doi: 10.1029/2004GL021002. URL http://dx.doi.org/10.1029/2004GL021002.

A.L. Gordon and J.C. Comiso. Polynyas in the southern ocean. *Scientific American; (USA)*, 258:6, Jun 1988.

Arnold L. Gordon. Oceanography: Southern ocean polynya. *Nature Clim. Change*, 4: 249–250, 4 2014.

Arnold L. Gordon, Martin Visbeck, and Josefino C. Comiso. A possible link between the weddell polynya and the southern annular mode*. *Journal of Climate*, 20:2558–2571, 6 2007.

Andrew McC. Hogg, Michael P. Meredith, Don P. Chambers, E. Povl Abrahamsen, Chris W. Hughes, and Adele K. Morrison. Recent trends in the southern ocean eddy field. *Journal of Geophysical Research: Oceans*, 120(1):257–267, 2015. ISSN 2169-9291. doi: 10.1002/2014JC010470. URL http://dx.doi.org/10.1002/2014JC010470.

John D. Horel and John M. Wallace. Planetary-scale atmospheric phenomena associated with the southern oscillation. *Monthly Weather Review*, 109(4):813–829, Apr 1981. ISSN 0027-0644. doi: 10.1175/1520-0493(1981)109⟨0813:PSAPAW⟩2.0.CO;2. URL http://dx.doi.org/10.1175/1520-0493(1981)109<0813:PSAPAW>2.0.CO;2.

Brian J. Hoskins and David J. Karoly. The steady linear response of a spherical atmosphere to thermal and orographic forcing. *Journal of the Atmospheric Sciences*, 38(6):1179–1196, Jun 1981. ISSN 0022-4928. doi: 10.1175/1520-0469(1981)038⟨1179:TSLROA⟩2.0.CO;2. URL http://dx.doi.org/10.1175/1520-0469(1981)038<1179:TSLROA>2.0.CO;2.

Helen L. Johnson and David P. Marshall. A theory for the surface atlantic response to thermohaline variability. *Journal of Physical Oceanography*, 32(4):1121–1132, Apr

2002. ISSN 0022-3670. doi: 10.1175/1520-0485(2002)032⟨1121:ATFTSA⟩2.0.CO;2. URL http://dx.doi.org/10.1175/1520-0485(2002)032<1121:ATFTSA>2.0.CO;2.

David J. Karoly. Southern hemisphere circulation features associated with el ni??o-southern oscillation events. *Journal of Climate*, 2(11):1239–1252, Nov 1989. ISSN 0894-8755. doi: 10.1175/1520-0442(1989)002⟨1239:SHCFAW⟩2.0.CO;2. URL http://dx.doi.org/10.1175/1520-0442(1989)002<1239:SHCFAW>2.0.CO;2.

Mitsuhiro Kawase. Establishment of deep ocean circulation driven by deep-water production. *Journal of Physical Oceanography*, 17(12):2294–2317, Dec 1987. ISSN 0022-3670. doi: 10.1175/1520-0485(1987)017⟨2294:EODOCD⟩2.0.CO;2. URL http://dx.doi.org/10.1175/1520-0485(1987)017<2294:EODOCD>2.0.CO;2.

Hannah Kleppin, Markus Jochum, Bette Otto-Bliesner, Christine A Shields, and Stephen Yeager. Stochastic atmospheric forcing as trigger for sudden greenland warmings. *J. Clim*, 2015. in review.

C. Lang, M. Leuenberger, J. Schwander, and S. Johnsen. 16 deg. c rapid temperature variation in central greenland 70,000 years ago. *Science*, 286(5441):934–937, 1999. doi: 10.1126/science.286.5441.934.

Shih-Yu Lee, John C. H. Chiang, Katsumi Matsumoto, and Kathy S. Tokos. Southern ocean wind response to north atlantic cooling and the rise in atmospheric co2: Modeling perspective and paleoceanographic implications. *Paleoceanography*, 26(1):n/a–n/a, 2011. ISSN 1944-9186. doi: 10.1029/2010PA002004. URL http://dx.doi.org/10.1029/2010PA002004.

Z. Liu, B. L. Otto-Bliesner, F. He, E. C. Brady, R. Tomas, P. U. Clark, A. E. Carlson, J. Lynch-Stieglitz, W. Curry, E. Brook, D. Erickson, R. Jacob, J. Kutzbach, and J. Cheng. Transient simulation of last deglaciation with a new mechanism for bølling-allerød warming. *Science*, 325(5938):310–314, 2009. doi: 10.1126/science.1171041.

V. Margari, L.C. Skinner, P.C. Tzedakis, A. Ganopolski, M. Vautravers, and N.J. Shackleton. The nature of millennial-scale climate variability during the past two glacial periods. *Nature Geoscience*, 3:127–133, 2010.

John Marshall and Kevin Speer. Closure of the meridional overturning circulation through southern ocean upwelling. *Nature Geosci*, 5(3):171–180, Mar 2012. ISSN 1752-0894. doi: 10.1038/ngeo1391. URL http://dx.doi.org/10.1038/ngeo1391.

Torge Martin, Wonsun Park, and Mojib Latif. Southern ocean forcing of the north atlantic at multi-centennial time scales in the kiel climate model. *Deep Sea Research Part II: Topical Studies in Oceanography*, 114(0):39 – 48, 2015. ISSN 0967-0645. doi: http://dx.doi.org/10.1016/j.dsr2.2014.01.018. URL http://www.sciencedirect.com/science/article/pii/S0967064514000320. Southern Ocean Dynamics and Biogeochemistry in a Changing Climate.

Darren C. McKee, Xiaojun Yuan, Arnold L. Gordon, Bruce A. Huber, and Zhaoqian Dong. Climate impact on interannual variability of weddell sea bottom water. *Journal of Geophysical Research: Oceans*, 116(C5):n/a–n/a, 2011. ISSN 2156-2202. doi: 10.1029/2010JC006484. URL http://dx.doi.org/10.1029/2010JC006484.

David R. Munday, Helen L. Johnson, and David P. Marshall. Eddy saturation of equilibrated circumpolar currents. *Journal of Physical Oceanography*, 43(3):507–532, Nov 2012. ISSN 0022-3670. doi: 10.1175/JPO-D-12-095.1. URL http://dx.doi.org/10.1175/JPO-D-12-095.1.

Larry C. Peterson, Gerald H. Haug, Konrad A. Hughen, and Ursula Röhl. Rapid changes in the hydrologic cycle of the tropical atlantic during the last glacial. *Science*, 290 (5498):1947–1951, 2000. doi: 10.1126/science.290.5498.1947.

S. Pond and G.L. Pickard. *Introductory Dynamical Oceanography*. Pergamon Press, 2nd edition, 1983.

Stefan Rahmstorf. A semi-empirical approach to projecting future sea-level rise. *Science*, 315(5810):368–370, 2007. doi: 10.1126/science.1135456. URL http://www.sciencemag.org/content/315/5810/368.abstract.

Robin Robertson, Martin Visbeck, Arnold L. Gordon, and E. Fahrbach. Long-term temperature trends in the deep waters of the weddell sea. *Deep Sea Research Part II: Topical Studies in Oceanography*, 49(21):4791 – 4806, 2002. ISSN 0967-0645. doi: http://dx.doi.org/10.1016/S0967-0645(02)00159-5. URL http://www.sciencedirect.com/science/article/pii/S0967064502001595. Deep Ocean Ventilation Through Antarctic Intermediate Layers (DOV ETAIL).

A. Schmittner, O.A. Saenko, and A.J. Weaver. Coupling of the hemispheres in observations and simulations of glacial climate change. *Quaternary Science Reviews*, 22(5–7):659 – 671, 2003. ISSN 0277-3791. doi: http://dx.doi.org/10.1016/

S0277-3791(02)00184-1. URL http://www.sciencedirect.com/science/article/pii/S0277379102001841.

Hartmut Schulz, Ulrich von Rad, and Helmut Erlenkeuser. Correlation between arabian sea and greenland climate oscillations of the past 110,000 years. *Nature*, 393(6680): 54–57, 1998. doi: 10.1038/31750. URL http://dx.doi.org/10.1038/31750.

T. Stocker and S. Johnsen. A minimum thermodynamic model for the bipolar seesaw. *Paleoceanography*, 18(1087), November 2003.

T. Stocker and F. Thomas. The seesaw effect. *Science*, 282(5386):61–62, 1998. doi: 10.1126/science.282.5386.61. URL http://www.sciencemag.org/content/282/5386/61.short.

Henry Stommel and A.B. Arons. On the abyssal circulation of the world ocean—i. stationary planetary flow patterns on a sphere. *Deep Sea Research (1953)*, 6(0):140 – 154, 1959–1960. ISSN 0146-6313. doi: http://dx.doi.org/10.1016/0146-6313(59)90065-6. URL http://www.sciencedirect.com/science/article/pii/0146631359900656.

Axel Timmermann, Laurie Menviel, Yuko Okumura, Annalisa Schilla, Ute Merkel, Oliver Timm, Aixue Hu, Bette Otto-Bliesner, and Michael Schulz. Towards a quantitative understanding of millennial-scale antarctic warming events. *Quaternary Science Reviews*, 29(1–2):74 – 85, 2010. ISSN 0277-3791. doi: http://dx.doi.org/10.1016/j.quascirev.2009.06.021. URL http://www.sciencedirect.com/science/article/pii/S0277379109002285. Climate of the Last Million Years: New Insights from {EPICA} and Other Records.

JR Toggweiler and B Samuels. Effect of drake passage on the global thermohaline circulation. *Deep Sea Research Part I: Oceanographic Research Papers*, 42(4):477–500, 1995.

Kevin E. Trenberth, Grant W. Branstator, David Karoly, Arun Kumar, Ngar-Cheung Lau, and Chester Ropelewski. Progress during toga in understanding and modeling global teleconnections associated with tropical sea surface temperatures. *Journal of Geophysical Research: Oceans*, 103(C7):14291–14324, 1998. ISSN 2156-2202. doi: 10.1029/97JC01444. URL http://dx.doi.org/10.1029/97JC01444.

H. Vanloon and D.J. Shea. The southern oscillation. part iv: The precursors south of 15°s to the extremes of the oscillation. *Monthly Weather Review*, 113:2063–2074, 1985. URL http://dx.doi.org/10.1175/1520-0493(1985)113%3C2063:TSOPIT%3E2.0.CO;2.

Antje H.L. Voelker. Global distribution of centennial-scale records for marine isotope stage (mis) 3: a database. *Quaternary Science Reviews*, 21(10):1185 – 1212, 2002. ISSN 0277-3791. doi: http://dx.doi.org/10.1016/S0277-3791(01)00139-1. URL http://www.sciencedirect.com/science/article/pii/S0277379101001391. Decadal-to-Millennial-Scale Climate Variability.

C. Waelbroeck, L. Labeyrie, E. Michel, J.C. Duplessy, J.F. McManus, K. Lambeck, E. Balbon, and M. Labracherie. Sea-level and deep water temperature changes derived from benthic foraminifera isotopic records. *Quaternary Science Reviews*, 21(1–3):295 – 305, 2002. ISSN 0277-3791. doi: http://dx.doi.org/10.1016/S0277-3791(01)00101-9. URL http://www.sciencedirect.com/science/article/pii/S0277379101001019. {EPILOG}.

Y. J. Wang, H. Cheng, R. L. Edwards, Z. S. An, J. Y. Wu, C.-C. Shen, and J. A. Dorale. A high-resolution absolute-dated late pleistocene monsoon record from hulu cave, china. *Science*, 294(5550):2345–2348, 2001. doi: 10.1126/science.1064618.

Carl Wunsch. Abrupt climate change: an alternative view. *Quat. Res*, 2006.